Photoproduction of K_S Pairs at GlueX
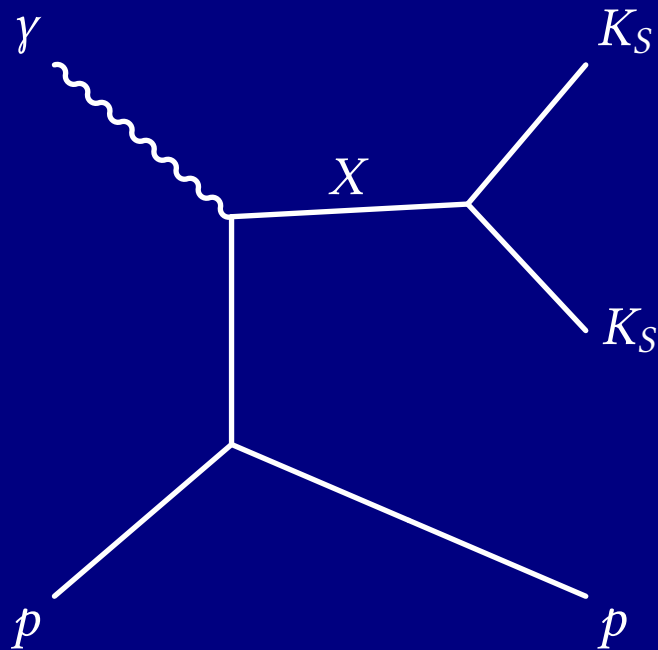
Nathaniel Dene Hoffman

Carnegie Mellon University

Table of Contents

Chapter 1

Introduction

1.1   A Brief History of Particle Physics

Since the days of the ancient Greeks, scientists and philosophers alike have been interested in the fundamental question concerning the composition of the universe. While the Greeks maintained that the world was composed of four indivisible elemental substances (fire, earth, air, and water) [1], this was at best a guess by the early philosophers, who had no mechanism with which to test their theory. Ironically, these philosophers struggled with a question to which us modern physicists still have no answer: Are the building blocks of the natural world fundamental (indivisible) [2]?

In 1808, John Dalton published a manuscript which described what is now called the "law of multiple proportions" after compiling several observations on chemical reactions which occur with specific proportions of their reactants. He anglicized the Greek *atomos*, meaning "not able to be cut", into the word we are familiar with—"atom" [3]. Towards the end of the century, J. J. Thomson demonstrated that cathode rays could be deflected by an electrostatic field, an observation which could not be explained by the prevailing theory that the rays were some form of light [4]. Instead, he proposed that these rays were made up of charged particles he called "corpuscles" (later renamed to the familiar "electrons") [5]. Around the same time (between 1906 and 1913), Ernest Rutherford, Hans Geiger, and Ernest Marsden conducted experiments in which they scattered alpha particles through a thin metal foil, and, through an analysis of the scattering angles, concluded that a positively charged nucleus must exist at the center of atoms, surrounded by electrons [6].

Over the next several decades, the nucleus was further divided into protons and neutrons[1] [7,8]. In 1964, Murray Gell-Mann and George Zweig proposed a theory that protons and neutrons (and all other baryons and mesons) were in fact composed of smaller particles Gell-Mann called "quarks" [9]. These particles, along with the electron-like

---

[1] For the discovery of the electron and neutron, Thomson and James Chadwick won Nobel Prizes in Physics in 1906 and 1935, respectively. Rutherford won the 1908 Nobel Prize in Chemistry for his research in radiation. However, I want to emphasize that while I mention the "big names" here, there are many who contributed in relative obscurity.

family of leptons (including neutrinos), the gauge bosons, and the Higgs boson, discovered in 2012 [10], comprise the Standard Model, a mathematical model which describes all the known forces and matter of the universe, with the notable exceptions (at time of writing) of gravity, dark matter, dark energy, and neutrino masses.

This thesis begins at a time when physicists are working hard to find gaps in this model, mostly by probing higher and higher ranges of energy. The experimental work being done at GlueX, however, resides in a lower energy regime, which we usually describe as "medium energy physics". As I will elucidate later in this manuscript, the strong force is non-perturbative in this regime, making direct calculations through the Standard Model all but impossible. However, since the advent of Lattice Quantum Chromodynamics (LQCD) in 1974 [11], physicists have been able to make approximate predictions via computer simulations of the theory.

1.2 Thesis Overview

Herein, I will focus on a particular portion of the Standard Model that dictates the strong interaction, viz. interactions between quarks and gluons, the mediating gauge boson of the strong force. Beginning with a discussion of the theory and history of K_S (K-short) pair production in prior experiments, I will give a brief overview of the GlueX experiment. I will then outline some of the theoretical underpinnings and implications of glueballs to persuade the reader on the importance of this production channel in the larger scheme of GlueX.

Next, I will describe my own analysis, beginning with the the impetus of this study, a search for Σ^+ baryons using a different recombination of the final state in this channel. This will lead to a first-order peek at the many resonances which decay to K_S pairs, and I will delineate the layers of data selection which I have carried out to produce a clean sample of events.

I will then discuss the process of partial-wave analysis (PWA), modeling resonances, and selecting a waveset for my data. I will conclude with the results from fits of these models to the data, the implications of such fits, and the next steps which I or another particle physicist might take in order to illuminate another corner of the light mesonic spectrum.

1.3 Motivation

While this will be discussed in detail later, I believe it is important to emphasize the motivation for such a study of photoproduction of $K_S K_S$. While the majority of GlueX research concerns the study of hybrid mesons (mesons with forbidden quantum numbers), such mesons cannot be found in this channel. Given a bound state of two spin-$\frac{1}{2}$ quarks with relative angular momentum L, total spin S and total angular momentum J (the eigenvalue of $\hat{J}^2 = \hat{L}^2 \oplus \hat{S}^2$), we

can define the parity operator $\hat{P}$ by its effect on the wave function of the system,

$$\hat{P}|\vec{r}\rangle = \eta|\vec{r}\rangle \tag{1.1}$$

where η can be determined by noting that states of angular momentum are generally proportional to a spherical harmonic in their angular distribution ($|r, \theta, \varphi; LM\rangle \sim Y_L^M(\theta, \varphi)$) and

$$\hat{P}Y_L^M(\theta, \varphi) = Y_L^M(\pi - \theta, \pi + \varphi) = (-1)^L Y_L^M(\theta, \varphi) \tag{1.2}$$

so $\eta = (-1)^L$. The Dirac equation can be used to show that the intrinsic parity of quarks and antiquarks, when multiplied, yields a factor of -1, so

$$\hat{P}|q\bar{q}; JLMS\rangle = -(-1)^L \tag{1.3}$$

Similarly, the operator $\hat{C}$ representing C-parity will also introduce a factor of $(-1)^L$ because exchanging charges of a (neutral[2]) quark-antiquark system is akin to reversing their positions under parity. If $|S\rangle$ is antisymmetric under C-parity, we should get an additional factor of -1, which is the case for the $S = 0$ singlet. With the aforementioned -1 due to the intrinsic parity of the quarks and antiquarks, we find

$$\hat{C}|q\bar{q}; JLMS\rangle = (-1)^{L+S} \tag{1.4}$$

Labeling states with the common J^{PC} notation, it can then be shown that states like 0^{--}, 0^{+-}, 1^{-+}, and 2^{+-} (among others) are not allowed states for $q\bar{q}$ mesons. As mentioned, the investigation of such states is the primary focus of the GlueX experiment. However, since the particle we are concerned with decays to two identical particles (K_S) which have a symmetric spatial wave function, and because this particle is a meson which follows Bose-Einstein statistics, the angular part of the total wave function must also be symmetric, i.e. $J =$ even integers. Furthermore, because parity is conserved in strong decays, and the state of two identical particles is symmetric under parity, the decaying meson must also have $P = +$. Finally, the strong interaction also conserves C-parity, and both kaons are neutral, so we can determine the J^{PC} quantum numbers of the resonance to be even^{++}. There should be no overlap here with the aforementioned hybrid mesons, but that does not mean the channel is not of interest to GlueX and the larger scientific community. Particularly, the lowest lying glueball states are predicted to not only share these quantum numbers, but exist in the middle of the mass range produced by GlueX energies [12]. To add to this, the spin-0 isospin-0 light flavorless mesons, denoted as f_0-mesons, are supernumerary, either due to mixing with a supposed light scalar glueball or by the presence of a light tetraquark (or both) [13].

However, it would be an understatement to say that the $K_S K_S$ channel at GlueX is not the ideal place to be looking for either glueballs or tetraquarks. This is because, while we have excellent handles for reconstructing this

---

[2]For $\hat{C}$ to be Hermitian, and thus observable, acting it twice on a state should return the original state, so only eigenvalues of ± 1 are allowed. Therefore, only states which are overall charge neutral are eigenstates of $\hat{C}$.

channel, we have no ability to separate particles of different isospin with these data alone. This means that these f states will be indistinguishable from their isospin-1 partners, the a-mesons. At first glance, it might seem like a model of the masses of these particles would make it easy to separate them, even if they remained indistinguishable between resonant peaks, but with broad states like the $f_0(1370)$ and states which sit right on top of each other (like the $f_0(980)$ and $a_0(980)$, which also tend to interfere with each other), there is likely no unique mass model which can distinguish all of the possible states without relying on data from other channels.

The silver lining is that, due to the GlueX detector's state-of-the-art angular acceptance [14], we do stand a chance at separating spin-0 states from spin-2 states, and GlueX's polarized beam allows us to further understand the mechanisms at play by giving us some indication of the parity of the t-channel exchanged particle in the production interaction. We can also use this channel as a proving ground for more complex amplitude analysis involving a mass model, which could be extended to a coupled-channel analysis in the future.

1.4   Past Analyses

This is certainly not the first attempt to study K_S^0 pair production. The earliest published experiment with a similar final state dates back to 1961, where researchers at CERN measured 54 events which ended in a final state which included two neutral kaons. Since only K_S^0 eigenstates decayed inside the bubble chamber, several of these early experiments infered a final state of $K_S^0 K_S^0$. For the majority of the 1960s and 1970s, research into this final state was dominated by pion beam production off a proton target, aside from a kaon beam experiment in 1977 (see Table 1.1). In the 1980s, several collaborations at DESY began studying electron-positron collisions, which imply an internal virtual photon fusion as the production mechanism. These experiments are an important counterpoint to those involving hadrons, since the glueball does not couple to photons, so any intermediate glueball production in these reactions should be heavily suppressed [15], although radial excitations should couple [16]. While the statistical power of these experiments was very small at first (relative to pion beam experiments), the L3 collaboration at LEP and Belle at KEKB provided larger data samples in the first two decades of the 2000s. Until this study, ITEP and BNL held the statistical lead in non-photon-fusion experiments, and we now present a dataset which is larger than both, even using the most restrictive selections of data.

There has only been one prior experiment, published by the CLAS collaboration in 2018 [17], which used photoproduction as a means of accessing this channel. While the "golden channel" for glueball production remains radiative J/ψ decays to $K_S^0 K_S^0 \gamma$, since non-glueball intermediate processes converting charm quarks into strange quarks are suppressed, photoproduction could be effective at creating exotic hybrid states as well as glueballs due via the photon's hadronic component or Pomeron exchange [16]. Additionally, the CLAS experiment did not utilize the polarized photon beam capability at JLab, but the current analysis at GlueX does, and this access to linear photon

Channel	Collaboration	# Events	Year
$\pi^- p \to K_S^0 K_S^0 n$	CERN/PS	54	1961 [18]
$\pi^- p \to K_S^0 K_S^0 n$	BNL	19	1962 [19]
$\pi^- p \to K_S^0 K_S^0 n$	LRL	66	1962 [20]
$\pi^- p \to K_S^0 K_S^0$ + neutrals	BNL	374	1966 [21]
$\pi^- p \to K_S^0 K_S^0 n$	LRL	426	1966 [22]
$\pi^- p \to K_S^0 K_S^0 n$	LRL	418	1967 [23]
$\pi^- p \to K_S^0 K_S^0 n$	CERN/PS	2559	1967 [24]
$\pi^- p \to K_S^0 K_S^0 n$	ANL/ZGS	1969	1968 [25] & 1969 [26]
$\pi^- p \to K_S^0 K_S^0 n$	CERN/PS	4820	1975 [27]
$\pi^- p \to K_S^0 K_S^0 n$	CERN/PS	6380	1976 [28]
$\pi^- p \to K_S^0 K_S^0 n$	ANL/ZGS	5096	1976 [29] & 1979 [30]
$K^- p \to K_S^0 K_S^0$ + neutrals	CERN/PS	410	1977 [31]
$\pi^- p \to K_S^0 K_S^0 n$	BNL/MPS	1278	1980 [32]
$\pi^- p \to K_S^0 K_S^0 n$	BNL/MPS	29381	1982 [33]
$e^+ e^- \to e^+ e^- K_S^0 K_S^0$	DESY/TASSO	100	1983 [34]
???	???	???	1986 (Bolonkin)
???	???	???	1986 (Baloshin)
$\pi^- p \to K_S^0 K_S^0 n$	BNL/MPSII	40494	1986 [35]
$e^+ e^- \to e^+ e^- K_S^0 K_S^0$	DESY/PLUTO	21	1987 [36]
$K^- p \to K_S^0 K_S^0 \Lambda$	SLAC/LASS	441	1988 [37]
$e^+ e^- \to e^+ e^- K_S^0 K_S^0$	DESY/CELLO	26	1988 [38]
$e^+ e^- \to e^+ e^- K_S^0 K_S^0$	LEP/L3	62	1995 [39]
$p p \to p p K_S^0 K_S^0$	Fermilab/E690	11182	1998 [40]
$\pi^- p \to K_S^0 K_S^0$ + neutrals	ITEP	$1000^\dagger$	1999 [41]
$e^+ e^- \to e^+ e^- K_S^0 K_S^0$	LEP/L3	802	2001 [15]
$\pi^- C \to K_S^0 K_S^0 + X$	ITEP	553	2003 [42]
$e^+ e^- \to e^+ e^- K_S^0 K_S^0$	LEP/L3	870	2006 [43]
$\pi^- p \to K_S^0 K_S^0 n$	ITEP	40553	2006 [44]
$e^+ e^- \to e^+ e^- K_S^0 K_S^0$	KEKB/Belle	$???^\ddagger$	2013 [45]
$\gamma p \to K_S^0 K_S^0 p$	JLAB/CLAS	$13500^\dagger$	2018 [17]
$\gamma p \to K_S^0 K_S^0 p$	JLAB/GlueX	65468^*	2025 (this analysis)

Table 1.1: Summary of all (known) past analyses involving production of K_S^0 pairs. Note that this is possibly not exhaustive and does not include any studies which focus on decays of an intermediate state, i.e. $J/\psi \to \gamma K_S^0 K_S^0$.
† - Estimated from plots.
‡ - Reported as three orders of magnitude larger than LEP's result from 2006, but an exact count was difficult to estimate.
* - Weighted number of events with KinFit $\chi_\nu^2 < 3.0$, the most restrictive selection used in this analysis (see Sections 2.1 and 2.2).

polarization can inform us of the parity exchanged in production of such exotic states. Our dataset is at least 4.8×

larger than what was used in this measurement.

Chapter 2

Experimental Design and Data Selection

2.1 The GlueX Experiment

GlueX, short for the Gluonic Excitation experiment located at the Thomas Jefferson National Accelerator Facility (JLab), first began collecting publication-ready data in 2016 with the goal of establishing the spectrum of light exotic states such as hybrid mesons and glueballs.

GlueX recieves an unpolarized electron beam from the Continuous Electron Beam Accelerator Facility (CEBAF), which is then converted to linearly polarized photons via coherent bremsstrahlung from a diamond radiator (see Figure 2.1). The scattering electrons are detected in an array of high-resolution scintillators called the Tagger Mi-
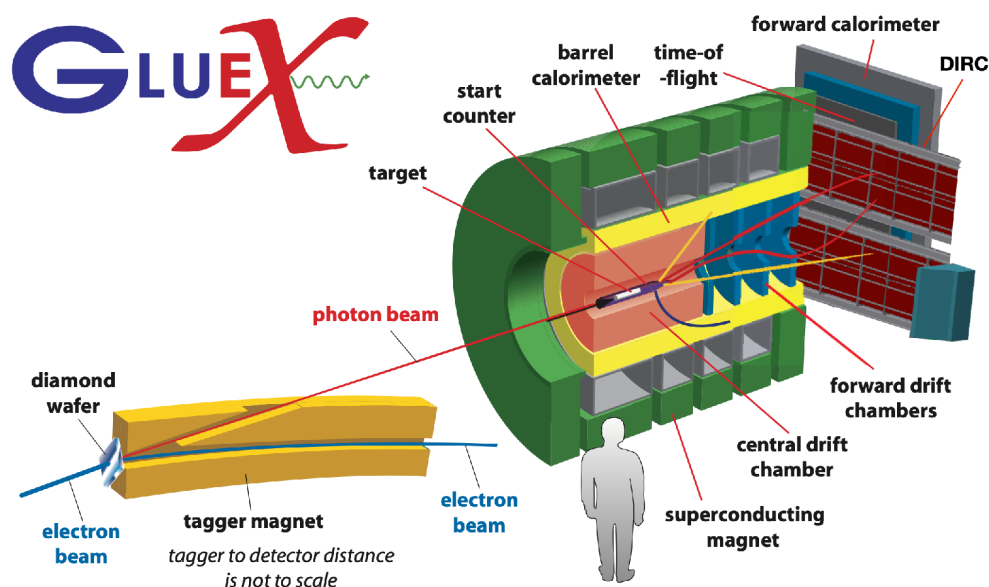

Figure 2.1: A diagram of the GlueX detector at JLab. The DIRC detector was installed in 2019 and was only present for about half of the data analyzed in this study.
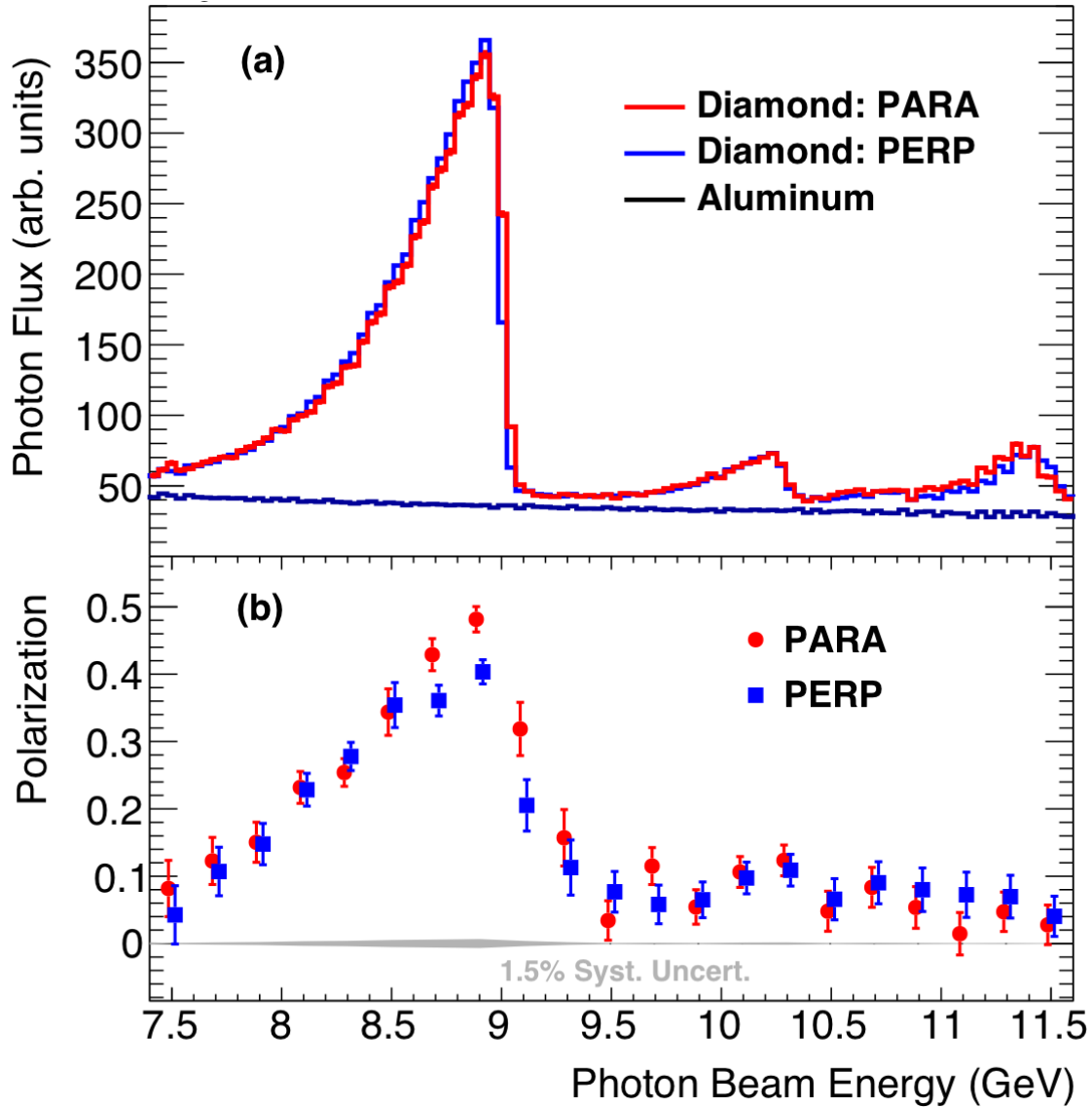
Figure 2.2: (a) Collimated photon beam intensity versus energy as measured by the Pair Spectrometer. (b) Collimated photon beam polarization as a function of beam energy, as measured by the Triplet Polarimeter, with data points offset horizontally by ±0.015 GeV for clarity. The labels PARA and PERP refer to orientations of the diamon radiator that result in polarization planes that are parallel and perpendicular to the horizontal, respectively (figure and caption from [14]).

croscope (TAGM) which covers beam energies between 8 and 9 GeV, a region of energy refered to as the "coherent peak". This range of beam energies has been specifically tuned (by modification of the radiator properties) to provide the highest amount of polarization (see Figure 2.2). The rest of the energy range, regions from about 3–8 GeV and 9–12 GeV, are covered by the lower-resolution Tagger Hodoscope (TAGM). These taggers are used to determine the photon energy, since it is equal to the difference between the incident and outgoing electron energies [14].

To measure the polarization properties of the photon beam as well as the photon flux, some portion of the photon beam passes through a thin beryllium foil which induces e^+e^- pair production (see Figure 2.3). The azimuthal angle
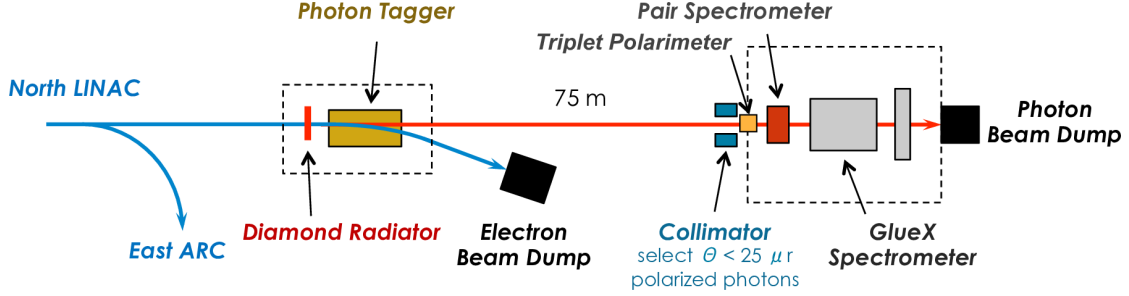
Figure 2.3: A diagram of the beamline layout of the Triplet Polarimeter (TPOL) and Pair Spectrometer (PS) used to measure the polarization and beam flux.

of the produced electrons is measured by the Triplet Polarimeter (TPOL) to measure the photon polarization. The Pair Spectrometer (PS) then counts these electrons in coincidence with the TAGM and TAGH detectors. A known fraction of the beam is converted to e^+e^- pairs in this way, allowing for an accurate measurement of the photon flux and the energy dependence of the polarization fraction.

Photons which were not passed into the TPOL/PS systems interact with a liquid hydrogen cryotarget, which maintains a temperature of 20.1 K, allowing the contents to act as a stationary proton target. A set of thin scintillators called the Start Counter (ST) surrounds the target, which captures the initial signals (and azimuthal angles) from reaction products and associates them with the electron radio frequency (RF) beam bunch from which the reaction originated. Any products of the reaction next pass through either the Central Drift Chamber (CDC) or Forward Drift Chamber (FDC) depending on their trajectory (particles moving along the direction of the beamline pass through the FDC). These chambers are filled with wires which sense the fields generated by charged particles as they pass nearby, allowing for the reconstruction of charged trajectories. The entire detector is situated inside a solenoid with a magnetic field around 2 T, and this field bends the trajectories of charged particles, allowing for proper identification of the sign of the charge as well as the particle's momentum. These chambers also allow for reconstruction of decay vertices by tracing back charged trajectories to their nearest approach.

The Barrel Calorimeter (BCAL) surrounding the CDC and the Forward Calorimeter (FCAL) in front of the FDC measure the energy of photon showers from interactions with charged and neutral particles. This includes photons

Experiment	Run Period	Luminosity ($E_\gamma > 6.0\,\text{GeV}$)	Coherent Peak Range	Luminosity in Coherent Peak
Phase-I	Spring 2017	$74.7\,\text{pb}^{-1}$	8.2–8.8 GeV	$21.8\,\text{pb}^{-1}$
	Spring 2018	$223.8\,\text{pb}^{-1}$	8.2–8.8 GeV	$63.0\,\text{pb}^{-1}$
	Fall 2018	$141.1\,\text{pb}^{-1}$	8.2–8.8 GeV	$40.1\,\text{pb}^{-1}$
Phase-II	Spring 2020	$386.2\,\text{pb}^{-1}$	8.0–8.6 GeV	$132.4\,\text{pb}^{-1}$
Total		$825.8\,\text{pb}^{-1}$		$257.3\,\text{pb}^{-1}$

Table 2.1: Summary of total luminosity and total luminosity in the coherent peak for each run period.

originating from the decays of light neutral mesons like the π^0 and η. Because such neutral particles pass through the CDC and FDC without detection, these calorimeters are necessary for their reconstruction. However, since only three vertices exist in such reconstructions (the initial vertex in the target and the final vertices in the calorimeter), GlueX is unable to reconstruct the decay vertices of these neutral particles. Since we are studying the a reaction with a fully charged final state, this might not seem important. However, in Section ?, we will discuss the study of neutral decays of $K_S^0 \to 2\pi^0 \to 4\gamma$, where the reconstruction will be severely limited due to the inability to reconstruct the decay vertex of the K_S^0.

There is a final scinatillator called the Time-of-Flight (TOF) detector situated immediately between the FDC and the FCAL. In combination with the ST, this aids in charged-particle identification via a measurement of the flight time between the two detectors. Additionally, in 2019, an additional detector, the DIRC[1] detector was installed between the TOF and FDC to further aid in identification of charged pions and kaons. This detector measures the angle of the cone of Cherenkov radiation emitted by relativistic charged particles, which can be used to ascertain their velocity via the relation $\cos\theta_c \sim 1/v$. When compared to measurements of the particle's momentum, this detector can be used to distinguish pions, kaons, and protons. Further information about the GlueX detector and the DIRC can be found in references [14] and [46] respectively.

The data analyzed in this thesis were collected in four separate "run periods" across two experiment "phases", denoted Phase-I and Phase-II. Phase-I consists of three run periods, notated Spring 2017, Spring 2018, and Fall 2018 by the season and year when data collection began, and Phase-II contains one run period, Spring 2020[2] and is the only dataset which was collected after the DIRC installation. The total luminosity, coherent peak range, and luminosity in the coherent peak for each run period is listed in Table 2.1.

The entire GlueX detector has been simulated with Geant4. Due to small changes and updates to the detector and its simulation between run periods, we will treat these datasets separately during the analysis, only presenting combined results in summary. Therefore, when generating Monte Carlo simulated data to model detector acceptance, each run period must be simulated separately.

---

[1]An acronym for Detection of Internally Reflected Cherenkov light
[2]This run technically began at the end of 2019

Particle Identification and the GlueX Kinematic Fit

Unsurprisingly, data collected from the GlueX detector mostly contains reaction topologies (the set of initial-, intermediate-, and final-state particles) which are not the channel of interest in this thesis. Additionally, due to the unavoidable finite resolution of each detector, the measured quantities such as the momentum of each particle might not exactly align with physical expectations (such as four-momentum conservation). For these reasons, we need to filter the detected data to just events which match our desired topology and kinematically fit the observables such as particle masses, decay vertices, and four-momenta with constraints that enforce conservation laws and other desirable properties.

This process begins with particle reconstruction, where the raw detector data is transformed into charged particle tracks (from the drift chambers), photon showers (from the calorimeters), and some timing data from the ST and TOF. Next, the charged tracks are matched up with their respective showers from the calorimeters, and the remaining showers are labeled as "neutral showers" originating from photons (or possibly large neutral particles like neutrons). At this stage, no particle identification is assigned to the charged and neutral tracks.

Particle Identification Cuts

The next stage involves filtering through reconstructed tracks to find events which match our topology. First, we apply some basic selections to the track data, including a requirement that neutral showers must have an energy of at least $100\,\mathrm{MeV}$ and neutral showers in the BCAL must be detected in at least two detector cells. Timing cuts are then applied to whichever detector gives the best timing information (the order being BCAL, TOF, FCAL, ST). By timing, we mean the difference between the time measured in the detector and the time of the RF beam bunch measured in the TAGH/TAGM. Each set of charged tracks is identified with each charged particle in the topology (events with too many or too few charged tracks are excluded). Each hypothetical identification is then subjected to cuts on the energy lost in the drift chambers or deposited in the calorimeters. Since there are no "missing" final-state particles (such as a neutron) in our reaction, an additional cut is made on the missing energy (the difference between the initial energy from the beam photon and the summed energy of the final-state particles). Finally, cuts are made on the invariant mass of some particles, as well as the missing mass (squared) for the step of the reaction from which the particle originated. For example, in the reaction $\gamma p \to K_S^0 K_S^0 p \to \pi^+\pi^-\pi^+\pi^- p$, a missing mass cut applied to the recoil proton would use the difference between the (squared) invariant mass of γp and $4\pi p$, but the missing mass cuts applied to one of th π^+ would involve the difference between the (squared) invariant mass of the K_S^0 it originated from and the decay product $\pi^+\pi^-$. A summary of these particle identification (PID) cuts can be seen in Table 2.2.

Particle	Selected Values	Unit	Detector
γ	$-1.5 \leq \Delta t_{\mathrm{RF}} \leq 1.5$	ns	BCAL
	$-2.5 \leq \Delta t_{\mathrm{RF}} \leq 2.5$	ns	FCAL
	$-0.1 \leq \mathrm{MM}^2 \leq 0.1$	$(\mathrm{GeV}/c^2)^2$	N/A
$\pi^{\pm}$	$-1.0 \leq \Delta t_{\mathrm{RF}} \leq 1.0$	ns	BCAL
	$-0.5 \leq \Delta t_{\mathrm{RF}} \leq 0.5$	ns	TOF
	$-2.0 \leq \Delta t_{\mathrm{RF}} \leq 2.0$	ns	FCAL
	$-2.5 \leq \Delta t_{\mathrm{RF}} \leq 2.5$	ns	ST
	$\frac{\mathrm{d}E}{\mathrm{d}x} < \exp\left[-7.0\left|\vec{p}\right| + 3.0\right] + 6.2$	keV/cm $\left(\frac{\mathrm{d}E}{\mathrm{d}x}\right)$, GeV/c $\left(\left|\vec{p}\right|\right)$	CDC
	$-1.0 \leq \mathrm{MM}^2 \leq 1.0$	$(\mathrm{GeV}/c^2)^2$	N/A
p	$-1.0 \leq \Delta t_{\mathrm{RF}} \leq 1.0$	ns	BCAL
	$-0.6 \leq \Delta t_{\mathrm{RF}} \leq 0.6$	ns	TOF
	$-2.0 \leq \Delta t_{\mathrm{RF}} \leq 2.0$	ns	FCAL
	$-2.5 \leq \Delta t_{\mathrm{RF}} \leq 2.5$	ns	ST
	$\frac{\mathrm{d}E}{\mathrm{d}x} > \exp\left[-4.0\left|\vec{p}\right| + 2.25\right] + 1.0$	keV/cm $\left(\frac{\mathrm{d}E}{\mathrm{d}x}\right)$, GeV/c $\left(\left|\vec{p}\right|\right)$	CDC
	$-0.5 \leq \mathrm{MM}^2 \leq 4.41$	$(\mathrm{GeV}/c^2)^2$	N/A
π^0	$0.08 \leq \mathrm{IM} \leq 0.19$	GeV/c^2	N/A
	$-1.0 \leq \mathrm{MM}^2 \leq 1.0$	$(\mathrm{GeV}/c^2)^2$	N/A
K_S^0	$0.3 \leq \mathrm{IM} \leq 0.7$	GeV/c^2	N/A
	$-1.0 \leq \mathrm{MM}^2 \leq 2.0$	$(\mathrm{GeV}/c^2)^2$	N/A
N/A	$-3.0 \leq \mathrm{ME} \leq 3.0$	GeV	N/A

Table 2.2: PID cuts used in event reconstruction. MM^2 corresponds to the missing mass squared, IM corresponds to the invariant mass, and *ME* corresponds to the total missing energy.

Kinematic Fit

The final stage of reconstruction invokes a kinematic fit (KinFit) over data which has passed all PID cuts. The general structure of the kinematic fit is underpinned by the following derivation from [?][3]. This kinematic fit minimizes the following objective function:

$$\chi^2(\vec{\eta}, \vec{\xi}) = (\vec{y} - \vec{\eta})^{\mathsf{T}} \mathbf{V}_{\vec{y}}^{-1} (\vec{y} - \vec{\eta}) + 2\vec{\lambda}^{\mathsf{T}} \vec{f}(\vec{\eta}, \vec{\xi}) \tag{2.1}$$

where $\vec{y}$ are the experimentally measured values of observables $\vec{\eta}$, $\mathbf{V}_{\vec{y}}$ is the covariance matrix of the measured $\vec{y}$, $\vec{f}(\vec{\eta}, \vec{\xi}) = 0$ are constraints applied to the system with additional free parameters $\vec{\xi}$ (which do not correspond to measured observables), and λ are unknown Lagrange multipliers for said constraints. Since we wish to minimize χ^2, we first take derivatives with respect to each set of free parameters,

$$\frac{\partial \chi^2}{\partial \vec{\eta}} = \mathbf{V}_{\vec{y}}^{-1}(\vec{\eta} - \vec{y}) + \left(\frac{\partial \vec{f}}{\partial \vec{\eta}}\right)^{\mathsf{T}} \vec{\lambda} \tag{2.2}$$

$$\frac{\partial \chi^2}{\partial \vec{\lambda}} = \vec{f}(\vec{\eta}, \vec{\xi}) \tag{2.3}$$

---

[3]How to cite GlueX docdb 2112?

$$\frac{\partial \chi^2}{\partial \vec{\xi}} = \left(\frac{\partial \vec{f}}{\partial \vec{\xi}} \right)^{\mathsf{T}} \vec{\lambda} \tag{2.4}$$

To find an extrema, we set these each to $\vec{0}$ and solve. At GlueX, the KinFit uses the Newton-Raphson method. First, we Taylor expand the constraint equations to first order,

$$\vec{f}(\vec{\eta}, \vec{\xi}) \approx \vec{f}(\vec{\eta}_0, \vec{\xi}_0) + \left(\frac{\partial \vec{f}}{\partial \vec{\eta}} \right) \bigg|_{\vec{\eta}_0, \vec{\xi}_0} (\vec{\eta} - \vec{\eta}_0) + \left(\frac{\partial \vec{f}}{\partial \vec{\xi}} \right) \bigg|_{\vec{\eta}_0, \vec{\xi}_0} \left(\vec{\xi} - \vec{\xi}_0 \right) \tag{2.5}$$

Assuming $\vec{\eta}_0$ and $\vec{\xi}_0$ are near the true minimum, we can set up an iterative method of approach,

$$\vec{f}_i + \left(\frac{\partial \vec{f}}{\partial \vec{\eta}} \right)_i (\vec{\eta}_{i+1} - \vec{\eta}_i) + \left(\frac{\partial \vec{f}}{\partial \vec{\xi}} \right)_i \left(\vec{\xi}_{i+1} - \vec{\xi}_i \right) = \vec{0} \tag{2.6}$$

where $\vec{f}_i \equiv \vec{f}(\vec{\eta}_i, \vec{\xi}_i)$, $\left(\frac{\partial \vec{f}}{\partial \vec{\eta}} \right)_i \equiv \left(\frac{\partial \vec{f}}{\partial \vec{\eta}} \right) \big|_{\vec{\eta}_i, \vec{\xi}_i}$, and $\left(\frac{\partial \vec{f}}{\partial \vec{\xi}} \right)_i \equiv \left(\frac{\partial \vec{f}}{\partial \vec{\xi}} \right) \big|_{\vec{\eta}_i, \vec{\xi}_i}$. To carry out an iteration, we need to determine the next step in each of the free directions $\vec{\eta}_{i+1}$ and $\vec{\xi}_{i+1}$. We start by writing the iterative forms of Equations (2.2) and (2.4) as

$$\mathbf{V}_{\vec{y}}^{-1} (\vec{\eta}_{i+1} - \vec{y}) + \left(\frac{\partial \vec{f}}{\partial \vec{\eta}} \right)_i^{\mathsf{T}} \vec{\lambda}_{i+1} = 0 \tag{2.7}$$

$$\left(\frac{\partial \vec{f}}{\partial \vec{\xi}} \right)_i^{\mathsf{T}} \vec{\lambda}_{i+1} = 0 \tag{2.8}$$

To obtain the next iterative estimate of $\vec{\eta}$ by rearranging Equation (2.7) as

$$\vec{\eta}_{i+1} = \vec{y} - \mathbf{V}_{\vec{y}} \left(\frac{\partial \vec{f}}{\partial \vec{\eta}} \right)_i^{\mathsf{T}} \vec{\lambda}_{i+1} \tag{2.9}$$

Inserting this back into Equation (2.6), we get

$$\vec{0} = \underbrace{\vec{f}_i + \left(\frac{\partial \vec{f}}{\partial \vec{\eta}} \right)_i (\vec{y} - \vec{\eta}_i)}_{\vec{r}_i} - \underbrace{\left(\left(\frac{\partial \vec{f}}{\partial \vec{\eta}} \right)_i \mathbf{V}_{\vec{y}} \left(\frac{\partial \vec{f}}{\partial \vec{\eta}} \right)_i^{\mathsf{T}} \right)}_{\mathbf{S}_i} \vec{\lambda}_{i+1} + \left(\frac{\partial \vec{f}}{\partial \vec{\xi}} \right)_i \left(\vec{\xi}_{i+1} - \vec{\xi}_i \right)$$

$$\vec{0} = \vec{r}_i - \mathbf{S}_i \vec{\lambda}_{i+1} + \left(\frac{\partial \vec{f}}{\partial \vec{\xi}} \right)_i \left(\vec{\xi}_{i+1} - \vec{\xi}_i \right)$$

$$\vec{\lambda}_{i+1} = \mathbf{S}_i^{-1} \left(\vec{r}_i + \left(\frac{\partial \vec{f}}{\partial \vec{\xi}} \right)_i \left(\vec{\xi}_{i+1} - \vec{\xi}_i \right) \right) \tag{2.10}$$

We can plug this definition of $\vec{\lambda}_{i+1}$ into Equation (2.8) to find the iterative update for $\vec{\xi}$:

$$\vec{0} = \left(\frac{\partial \vec{f}}{\partial \vec{\xi}}\right)_i^{\mathsf{T}} \mathbf{S}_i^{-1} \vec{r}_i + \underbrace{\left(\frac{\partial \vec{f}}{\partial \vec{\xi}}\right)_i^{\mathsf{T}} \mathbf{S}_i^{-1} \left(\frac{\partial \vec{f}}{\partial \vec{\xi}}\right)_i}_{\mathbf{U}_i} \left(\vec{\xi}_{i+1} - \vec{\xi}_i\right)$$

$$\vec{\xi}_{i+1} = \vec{\xi}_i - \mathbf{U}_i^{-1} \left(\frac{\partial \vec{f}}{\partial \vec{\xi}}\right)_i^{\mathsf{T}} \mathbf{S}_i^{-1} \vec{r}_i \tag{2.11}$$

To perform the kinematic fit, we use the available measured observables and their covariances (contained in $\vec{r}$, $\mathbf{S}$, and $\mathbf{U}$) to update our estimate of $\vec{\xi}$ via Equation (2.11). Next, we use that result to update $\vec{\lambda}$ via Equation (2.10). Finally, we update $\vec{\eta}$ via Equation (2.9). This process is repeated until the desired precision of these variables is met, and is guaranteed to converge as long as the initial values start near the minimum. The χ^2 value obtained from evauating Equation (2.1) on the converged values tells us the quality of the fit. See Figure 2.4 for the distribution of $\chi_\nu^2 \equiv \chi^2/\nu$, where ν is the number of degrees of freedom in the fit, for both the real data and Monte Carlo simulation of the signal.

The constraints $\vec{f}$ used in this channel include four-momentum conservation,

$$\sum_{f\in\text{final}} p_f^\mu - \sum_{i\in\text{initial}} p_i^\mu = 0^\mu \tag{2.12}$$

where the sum over four-momenta of of the initial-state particles must match that of the final-state particles, and the masses of each intermediate K_S^0,

$$p_{K_S^0}^2 - m_{K_S^0}^2 = 0 \tag{2.13}$$

where $m_{K_S^0}$ is the known mass of the K_S^0 and $p_{K_S^0}$ is the fitted estimate of the four-momentum reconstructed from the $\pi^+\pi^-$ four-momentum measured by the detectors. Additionally we constrain the initial and final positional vertices of each production step in the topology. For this channel, this means we constrain the initial production vertex and the point of closest approach of the K_S^0s and recoil proton, as well as the decay vertex of each K_S^0 with the closest approach of its constituent pions. It is important to note that this vertex constraint cannot be done in the case where a K_S^0 decays to $2\pi^0$, since the neutral pions will decay to 2γ which can only be detected the calorimeters. Because there is not a second point of detection for these photons, their trajectory and therefore the point at which the original π^0 decayed is unknown, so there is no way to further reconstruct the kaon decay vertex because the point of closest approach is unknown[4]. Therefore, when we specify channels where one or both kaons decay as $K_S^0 \to 2\pi^0$, we do not include these K_S^0s in the kinematic fit at all, and must infer them by adding the π^0 four-momenta (see SECTION). For the main $\gamma p \to K_S^0 K_S^0 p \to 2\pi^+ 2\pi^- p$ channel, we have four constraints from four-momentum

---

[4]The best we could do would be to assume the kaon decayed at the initial reaction vertex inside the target, which is not only unrealistic given that kaons decay via the weak interaction, but also causes problems later when we try to calculate the kaon lifetime to use in event weighting in Section 2.3.
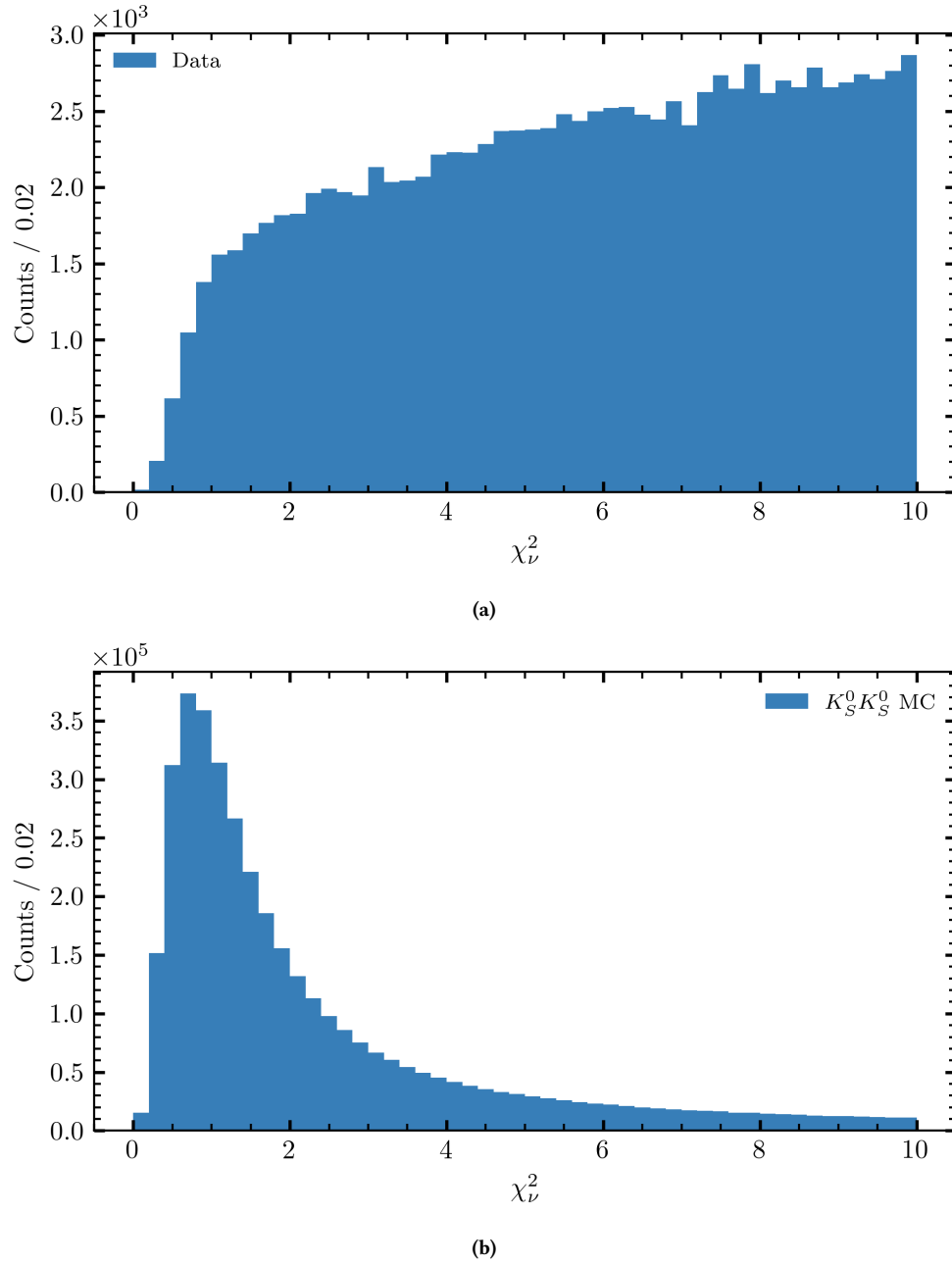
(a)

(b)

Figure 2.4: Distributions of χ^2_ν (the χ^2 per degree of freedom of the GlueX kinematic fit) for (a) data and (b) signal Monte Carlo after reconstruction cuts but before any fiducial selections from Section 2.2. Note that the data extends past $\chi^2_\nu > 10$, but the plot was truncated for legibility. Both datasets have had accidental subtraction applied and combos flattened (see Sections 2.1 and 2.2).

conservation, two mass constraints (one for each kaon), 14 vertex constraints (two for each constrained particle, viz. four pions, two kaons, and a proton), and nine unknowns from the vertex constraints (the position of the vertex introduces three unknowns for each vertex, and there are three constrained vertices, viz. two kaon decays and the initial production vertex). This gives a total of 20 constraints with nine unknowns, or 11 degrees of freedom in the fit.

Combos

While the initial interaction vertex in theory contains a single photon, in practice, the incident beam contains multiple tagged photons, any of which might provide the requisite energy needed to kinematically generate a given set of final-state tracks. Additionally, there could be multiple ways to recombine or identify final-state particles to arrive at the same event topology. The GlueX reconstruction process considers all valid combinations of tagged photons and sets of reconstructed final-state particles and saves each one in a sub-event called a "combo". Each event has at least one of these combos, and some events may have many due to there being many candidate beam photons with similar energies. Since only one combo can be the true event, we need to flatten the data in a way that avoids double counting events. The method for doing so is discussed in SECTION.

2.2   Data Selection for the $K_S K_S$ Channel

Fiducial Cuts

2.3   sPlot Weighting

At this stage in the analysis, we have no more simple cuts which can improve the signal-to-background ratio in the dataset, but we know there must still be background remaining, as is indicated by the excess events with small kaon rest-frame lifetimes seen in Figure 2.5. In this figure, we see that one of the intrinsic properties of a K_S^0, its well-known lifetime, is not distinct in the data. Rather, we seem to have at least two exponential slopes in the rest-frame lifetime distribution of each kaon, one which is close to what we see in signal Monte Carlo, and another which is similar to the 4π background Monte Carlo. We must now turn to more complex methods of separating the signal from this potential background seepage. The primary method we will use to do this is sPlot [47][5], a weighting scheme which corrects the naïve probabilistic weights one might first think to construct (dubbed "inPlot"). We begin by giving a basic explanation of inPlot before describing the sPlot correction.

For all of the statistical weighting methods which will be mentioned here, we need some model for the signal and background probability distribution functions (PDFs) for some "discriminating" variable. This variable is called

---

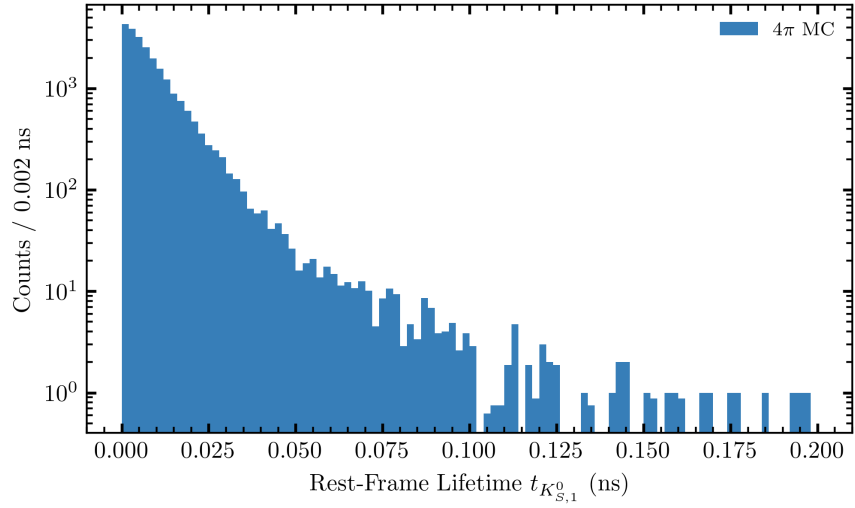[5]This is stylized as $_sPlot$ in the original paper, but I find this tedious to type and to read.
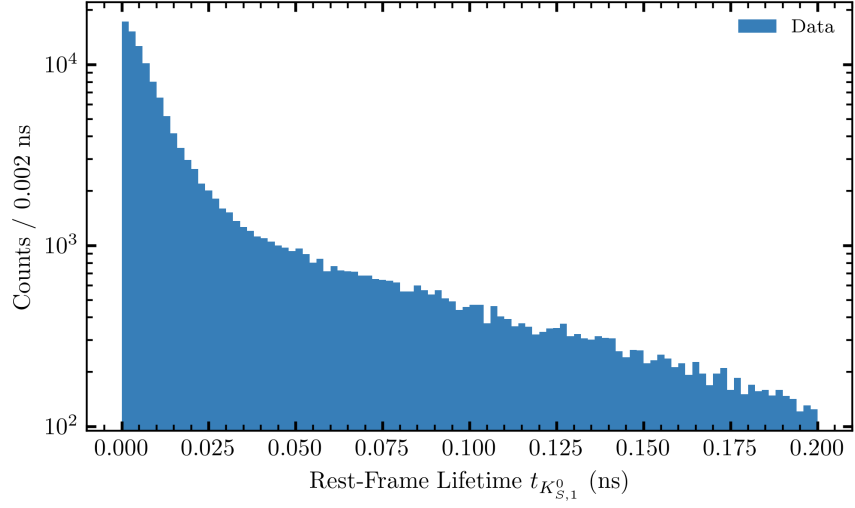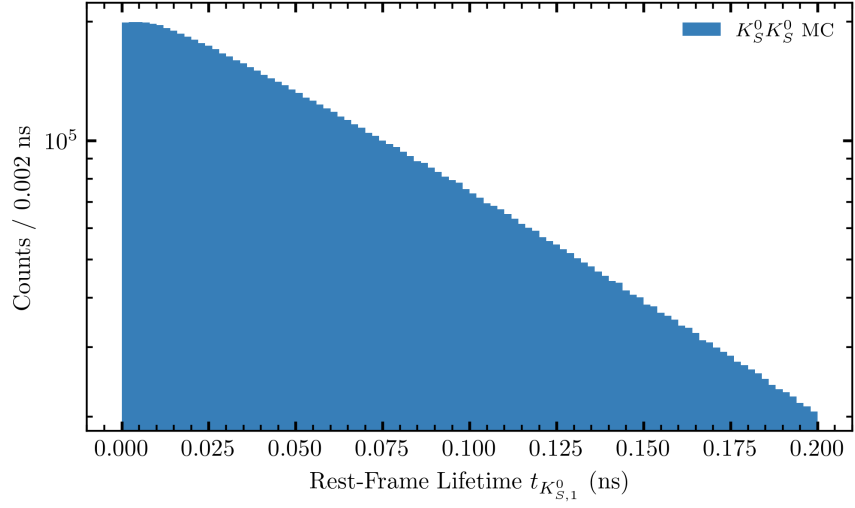
Figure 2.5: The rest-frame lifetime of kaons in (a) data, (b) signal Monte Carlo, and (c) background Monte Carlo. The data distribution clearly contains two exponential slopes: a peak which resembles the 4π Monte Carlo distribution, and a tail of true K_S^0s which resembles the signal Monte Carlo.

"discriminating" because it the variable for which we know the shape of these distributions beforehand. The usual example is a "bump-on-a-background", in which the discriminating variable may be a mass distribution (m) where signal events show up as a peaking structure while background events are more uniformly distributed. In such situations, it is common to use the extremes of the mass distribution (sidebands) as estimates of the background everywhere, weighting these events negatively while the events in the peak are weighted positively (a sideband subtraction). Rather than specifying peak and sideband regions, we can fit the mass distribution to some mixture of a signal (peak) PDF $f_S(m)$ and a background (flat) PDF $f_B(m)$. From such a fit, we obtain estimated number of signal (N_S) and background (N_B) events in our dataset (and possibly some shape parameters for the signal and background PDFs). We could then assign weights to each event as in Equation (2.14),

$$w(m) = \frac{N_S f_S(m)}{N_S f_S(m) + N_B f_B(m)} \tag{2.14}$$

We might want to look at the "signal" inPlots for the decay angles θ and φ (control variables) in the helicity system after calculating the inPlot weights from a fit to the mass distribution (discriminating variable). However, as shown by Pivk and Le Diberder [47], we can only use inPlot in cases where the control variables are totally correlated with the discriminating variable[6] y. In other words, our example would only be valid if $\theta = \theta(m)$ and $\phi = \phi(m)$. For the time being, let us assume that this is not the case, and that we wish to use the distribution of some variable which is totally uncorrelated with the variables we are plotting and analyzing[7]. A correction term can be applied to give us the sPlot version of Equation (2.14),

$$w(y) = \tilde{w}(y) \frac{V_{SS} f_S(y) + V_{SB} f_B(y)}{N_S f_S(y) + N_B f_B(y)}, \quad \text{where } V_{ij}^{-1} = \sum_y \frac{\tilde{w}(y) f_i(y) f_j(y)}{(N_S f_S(y) + N_B f_B(y))^2} \tag{2.15}$$

where y represents any set of discriminating variables (not necessarily a mass), and $\tilde{w}(y)$ is any pre-existing weight associated with the event (weights from accidental subtraction, for instance). The V^{-1} matrix can also be understood as the covariance matrix between the free parameters N_S and N_B in the fit of the signal-background mixture, $V_{ij}^{-1} = -N \frac{\partial^2 \ln \mathcal{L}}{\partial N_i \partial N_j}$, although there is reason to believe that direct calculation by inverting the Hessian matrix from the fit will lead to less accurate results than the manual calculation method given in Equation (2.15) [48].

Now that we have a method of assigning weights, we must pick the discriminating variables. As mentioned, these weighting methods work well on the classic "bump-on-a-background" distributions because it is easy to identify the signal and background PDFs, but because the mass of the kaons is constrained in the kinematic fit, the fitted mass of each kaon is just a δ-function and combination of measured masses for each $\pi^+ \pi^-$ pair will yield a Normal distribution with little to no apparent background (by construction), so we must be a bit more clever in selecting

---

[6]In practice, more than one discriminating variable can be used.
[7]Total (un)correlation is a very strict requirement, but we will later see that small modifications to the sPlot method can permit amounts of correlation between the two extremes.

discriminating variables. By examining the BGGEN analysis done in [TODO: PREVIOUS SECTION], we can see that most likely sources of background arise when the intermediate kaons are absent from the reaction: $\gamma p \to 4\pi p$. This reaction has the $K_S K_S$ final state, so pairs of pions which reconstruct close enough to kaons will be almost indistinguishable in the data. However, they differ in one key way, namely that the K_S intermediate contains a strange quark while the $\pi^+ \pi^-$ decay state does not, so such a decay must occur via the weak interaction, which is notably slower than the strong interaction which would produce pion pairs with no intermediate kaon. In other words, while the signal's rest-frame lifetime distribution should have an exponential slope near the K_S lifetime, the background would theoretically have nearly zero rest-frame lifetime for every event, or a much smaller exponential slope in practice[8].

Therefore, we will begin by generating both a signal and background dataset in Monte Carlo. We then interpret both datasets as if they were our desired channel by running them through the GlueX reconstruction and reaction filter, as well as all of our selections up to this point. We can then fit the rest-frame lifetime of each dataset to an exponential model,

$$f(t; \lambda) = \lambda \exp\{-\lambda t\} \tag{2.16}$$

where $\lambda \equiv 1/\tau$, the lifetime of the kaon in question. Since we have two independently decaying kaons, we should really form a joint distribution for both, where we will assume each kaon has the same average lifetime:

$$f(t_1, t_2; \lambda) = \lambda^2 \exp\{-\lambda t_1\} \exp\{-\lambda t_2\} \tag{2.17}$$

Both the signal and background distributions can be modeled in this way, giving us only two free parameters, λ_S and λ_B for the signal and background respectively, to fit.

We can then use a mixture of exponential distributions with both signal and background slopes to fit the entire dataset:

$$f(t_1, t_2; z, \lambda_S, \lambda_B) \equiv z f(t_1, t_2; \lambda_S) + (1 - z) f(t_1, t_2; \lambda_B) \tag{2.18}$$

where z is the signal fraction of the total number of events N. From its fit value, we can determine values of $N_S = z \cdot N$ and $N_B = (1 - z) \cdot N$ to use in Equation (2.15) and complete the weighting procedure. We can perform this fit by minimizing the negative log-likelihood function,

$$-2 \ln \mathcal{L}(z, \lambda_S, \lambda_B) = -2 \sum_i^N \tilde{w}_i \ln f(t_{1,i}, t_{2,i}; z, \lambda_S, \lambda_B) \tag{2.19}$$

where again, we include any pre-existing weights $\tilde{w}$ in the fit.

---

[8]An exponential distribution is just what best fits the rest-frame lifetime distribution in the 4π Monte Carlo and has no physical implication.

Non-Factorizing sPlot

Over the course of the previous discussion, it was assumed that the discriminating variables, t_1 and t_2, were statistically independent from the control variables we wish to use in later analyses. The set of control variables must include all variables we use as inputs to the partial-wave analysis in Chapter 3, including the invariant mass m of the $K_S^0 K_S^0$ system and the helicity angles θ and φ of the decay. We should now confirm that the rest-frame lifetimes are totally uncorrelated with these control variables (in other words, show that they are statistically independent). To test for statistical independence between $t_{1,2}$ and a given control variable, we first split our dataset into M evenly-spaced quantiles in that control variable, which ensures each bin gets roughly the same number of events. Next, we calculate the likelihood of a null hypothesis which assumes the variables are statistically independent by fitting all datasets simultaneously with shared λ_S and λ_B parameters. We then calculate the likelihood of an alternative hypothesis, which assumes statistical dependence, by finding the joint likelihood of independent fits of λ_S and λ_B over each quantile. The result of these fits can be formulated as a likelihood ratio,

$$\Lambda = -2 \ln \frac{\sup \mathcal{L}_{H_0}}{\sup \mathcal{L}_{H_1}} = -2 \ln \frac{\sup \prod_i^M \mathcal{L}_i(z_i, \lambda_S, \lambda_B)}{\sup \prod_i^M \mathcal{L}_i(z_i, \lambda_{S,i}, \lambda_{B,i})} \tag{2.20}$$

where $\mathcal{L}_{H_0}$ and $\mathcal{L}_{H_1}$ are the likelihoods of the null and alternative hypotheses respectively, the supremum indicates we are maximizing these likelihoods (in a maximum likelihood fit), the product $\prod_i^M$ iterates over each quantile of data in the given control variable, and $\mathcal{L}_i$ is the likelihood evaluated over data in the ith quantile. Λ is χ^2 distributed with $2M - 2$ degrees of freedom (the difference between $M + 2$ free parameters in the null hypothesis, a signal fraction z_i for each quantile plus the two exponential slopes shared across all quantiles, and $3M$ in the alternative hypothesis, a signal fraction and two exponential slopes for each quantile). The factor of 2 is required because $\ln \mathcal{L}(\theta_1, ..., \theta_i) \sim -\frac{1}{2}\chi_i^2$ asymptotically with sample size, according to Wilks' theorem. We can obtain a p-value representing the likelihood of the null hypothesis being true by evaluating the p-value:

$$p = 1 - F_{\chi^2_{2M-2}}(\Lambda) \tag{2.21}$$

where $F_{\chi^2_{2M-2}}(\Lambda)$ is the cumulative distribution function of a χ^2 distribution with $2M - 2$ degrees of freedom. Following this procedure for the invariant mass of $K_S^0 K_S^0$[9], the p-values for each number of quantiles can be seen in the first row of Table 2.3 and in Figure 2.6, which depicts the case with four quantiles. The calculated p-values tend to be very small, implying that we should reject the null hypothesis and accept that the discriminating (rest-frame lifetime) and control (invariant mass of $K_S^0 K_S^0$) variables are not statistically independent. This means we cannot use a traditional sPlot to weight our data.

---

[9]No significant statistical dependence was found for the helicity angles.

	# quantiles		
	2	3	4
Data Type	p	p	p
Data	1.26×10^{-101}	9.94×10^{-103}	4.49×10^{-112}
$K_S^0 K_S^0$ MC	$< 2.23 \times 10^{-308}$	$< 2.23 \times 10^{-308}$	$< 2.23 \times 10^{-308}$
4π MC	1.87×10^{-05}	1.00×10^{-04}	7.38×10^{-05}

Table 2.3: The probability of accepting the null hypothesis (that the rest-frame lifetime is statistically independent of the invariant mass of $K_S^0 K_S^0$) for the tests described in Equation (2.20) for data and Equation (2.23) for Monte Carlo with the given number of quantiles. All values are calculated with a $\chi_\nu^2 < 3.0$ selection on each type of data over all run period combined. Values listed as $< 2.23 \times 10^{-308}$ are nonzero but smaller than the smallest representable 64-bit floating point number

Fortunately, the process for obtaining the correct weights is straightforward, we simply allow for more than one signal and background component in the fit and sum over all signal components when we calculate the final weight values [48]. Since the weights corresponding to each signal component in the sPlot can be added to each other to obtain a joint weight [47], Equation (2.15) can be extended to allow multiple signal and background components:

$$w(x) = \frac{\sum_j V_{S_0 j} f_j(x)}{\sum_k N_k f_k(x)} + ... + \frac{\sum_j V_{S_n j} f_j(x)}{\sum_k N_k f_k(x)}, \quad \text{where } V_{ij}^{-1} = \sum_x \frac{f_i(x) f_j(x)}{\left(\sum_k N_k f_k(x)\right)^2} \tag{2.22}$$

and S_i are the indices of the signal components.

We can further verify the need for non-factorizing sPlot by performing the factorization test described in Equations (2.20) and (2.21) to the signal and background Monte Carlo, with a slight modification to the number of free parameters, since we only need to fit either a signal or background component rather than a mixture:

$$p = 1 - F_{\chi_{M-1}^2} \quad \text{where } \Lambda = -2 \ln \frac{\sup \prod_i^M \mathcal{L}_i(\lambda)}{\sup \prod_i^M \mathcal{L}_i(\lambda_i)} \tag{2.23}$$

The results of these tests over the signal and background Monte Carlo can also be found in the last two rows of Table 2.3 and are visualized for four quantiles in Figure 2.7. Again, the significantly small p-values justify the use of non-factorizing sPlot across both the signal and background components, meaning that we need at least two signal and two background components in the final sPlot weighting.

Application of Weights

The only thing left to do is determine how many signal and background components we should use in the weighting procedure. To this end, we now turn to the Monte Carlo simulations of the signal and 4π-background. By choosing a number of quantiles in invariant mass corresponding to the number of components, we can fit single exponential distributions to each quantile in the simulated signal and background. For instance, if we chose to use two signal components and three background components, we would divide the signal Monte Carlo into two quantiles and the
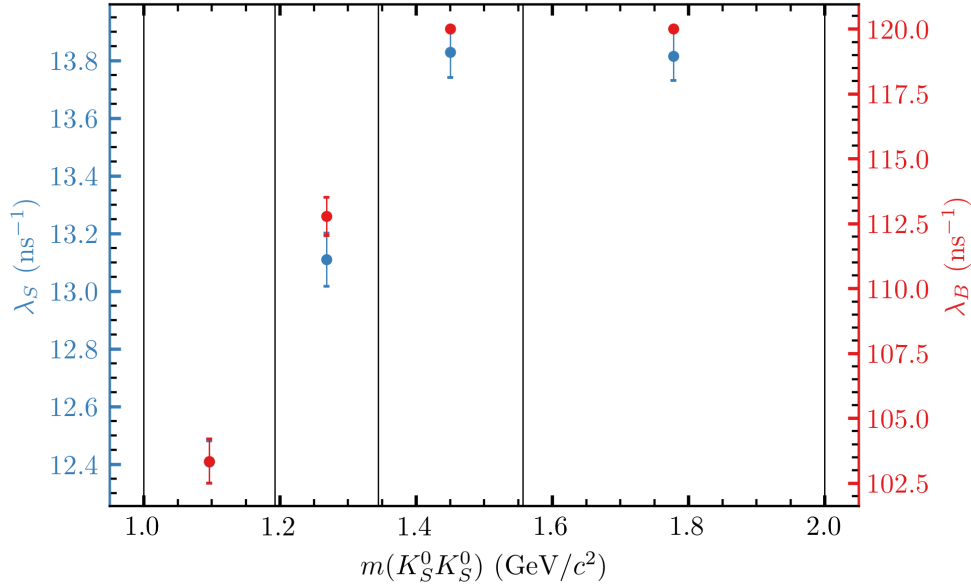
Figure 2.6: Exponential slopes from fits over four quantiles in $m(K_S^0 K_S^0)$ (x-axis) to a mixture of signal (left y-axis) and background (right y-axis) components. These fits show a definite statistical dependence between rest-frame lifetime and the invariant mass of $K_S^0 K_S^0$, as described in Table 2.3. All values are calculated with a KinFit $\chi_\nu^2 < 3.0$ selection on each type of data over each run period.

background Monte Carlo into three, and fit each quantile to an exponential distribution to obtain a set of two λ_S and three λ_B values. The resulting λ_S and λ_B values could then be used as a starting point for a multi-component fit to the data. Alternatively, both the signal and background or just the signal could be fixed to the values from the fits to simulations, and only the yields (or the yields and background λs) would be allowed to float in the fit to data. We will refer to the first case, where the fit parameters from Monte Carlo are free, as A, the case where the signal λs are fixed as B, and the case where all λs are fixed (and the only floating parameters are the yields of each component) as C. To select a model, we can use the relative Akaike Information Criterion (AIC) [49] and Bayesian Information Criterion (BIC) [50]:

$$r\text{AIC} \equiv \text{AIC} - \text{AIC}_{\text{min}} \quad \text{where AIC} \equiv 2k - 2\ln\mathcal{L} \tag{2.24}$$

$$r\text{BIC} \equiv \text{BIC} - \text{BIC}_{\text{min}} \quad \text{where BIC} \equiv k\ln N - 2\ln\mathcal{L} \tag{2.25}$$

$$\tag{2.26}$$

where k is the number of free parameters and N is the number of events in the dataset. The optimal model will minimize these criteria. In Table 2.4, all of the relative AIC and BIC values are shown. Excluding cases with only one signal or background component (restricting to models which have non-factorizing signal and background components), the minimizing values for most run periods tend to use two or three signal and two background components, and they both use method B, where the signal components are fixed to values obtained from Monte Carlo while

(a)

(b)

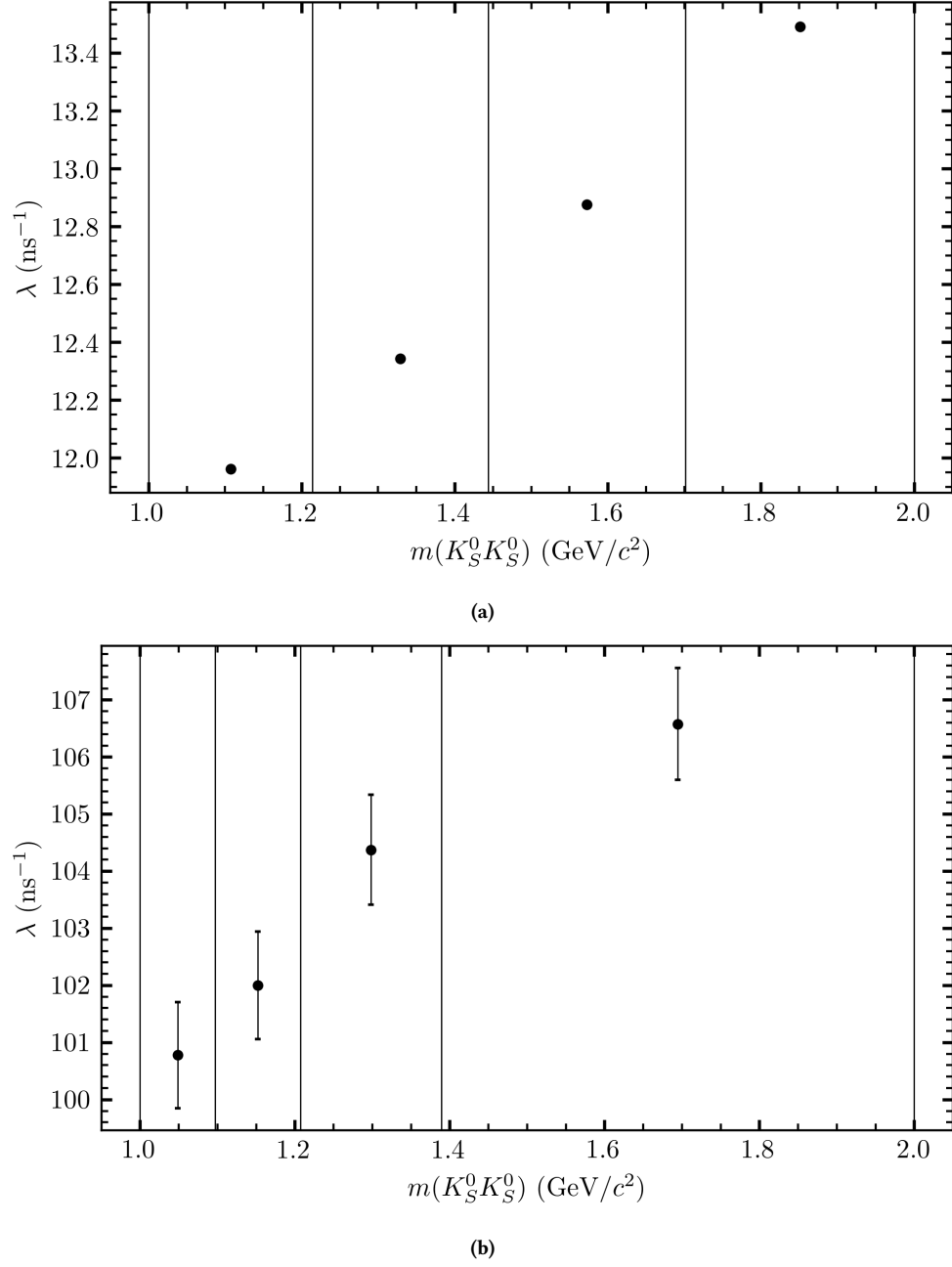**Figure 2.7:** Exponential slopes from fits over four quantiles in $m(K_S^0 K_S^0)$ (x-axis) of the (a) signal and (b) background Monte Carlo rest-frame lifetime distributions. Both show a definite statistical dependence between rest-frame lifetime and the invariant mass of $K_S^0 K_S^0$, as described in Table 2.3. All values are calculated with a KinFit $\chi_\nu^2 < 3.0$ selection on each type of data over each run period.

| Method | # Components | | rAIC | rBIC |
	Signal	Background		
A	1	1	<u>0.000</u>	<u>0.000</u>
	1	2	4.000	25.420
	1	3	8.004	50.843
	2	1	4.000	25.420
	2	2	8.000	50.839
	2	3	12.003	76.261
	3	1	8.000	50.839
	3	2	12.002	76.261
	3	3	16.002	101.681
B	1	1	312.365	301.655
	1	2	213.928	224.638
	1	3	217.324	249.453
	2	1	23.929	23.929
	2	2	9.758	$\boxed{31.177}$
	2	3	13.629	56.468
	3	1	2.001	12.711
	3	2	$\boxed{6.004}$	38.134
	3	3	10.002	63.551
C	1	1	1695.033	1673.614
	1	2	1305.143	1294.433
	1	3	1197.528	1197.528
	2	1	1661.600	1650.890
	2	2	1245.238	1245.238
	2	3	1128.344	1139.053
	3	1	1661.070	1661.070
	3	2	1247.365	1258.074
	3	3	1131.169	1152.588

Table 2.4: Relative AIC and BIC values for each fitting method. The absolute minimum values in each column are underlined, and the minimums excluding models with only one signal or background component are boxed.

the background components are initialized at Monte Carlo values but allowed to float in the fit. We will use the minimal non-factorizing model, method B with two signal and two background components, denoted $B(2, 2)$, as our weighting method. See Figure 2.8 for the result of this fit. The selection of method B is also interesting as it could describe a case where another background which is not modeled in the background Monte Carlo is present and has a similar exponential slope. Since these slopes are free in the fit to the data, they may anticipate this unknown slope better than the fixed case (method C), and method B also explicitly assumes the Monte Carlo for true signal kaons is correct and fixes their component slopes (unlike method A).
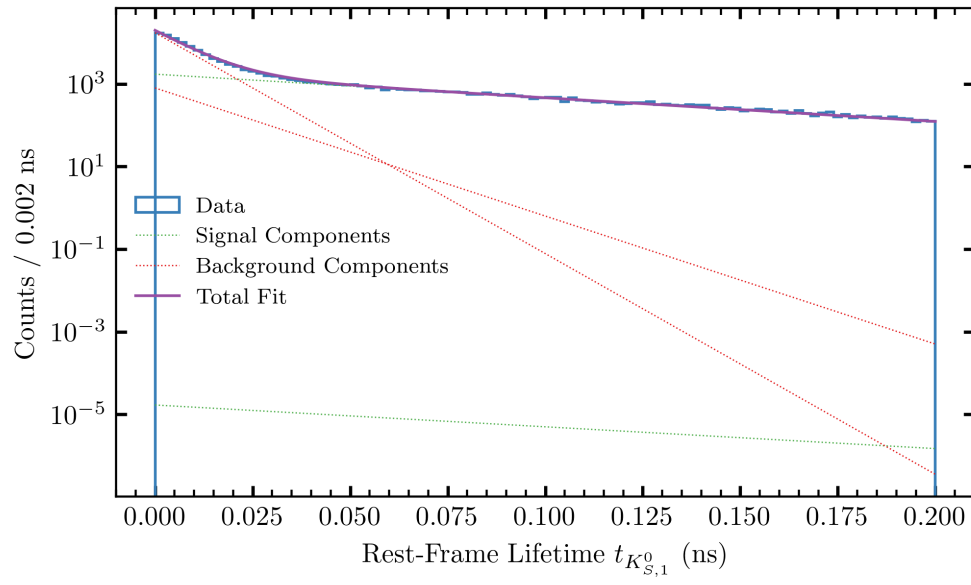
Figure 2.8: Fit of Equation (2.18) to data using method $B(2,2)$. True kaon events are prominent in the tail of the distribution, whereas background events peak strongly near zero. All values are calculated with a KinFit $\chi^2_\nu < 3.0$ selection on each type of data over each run period. The second signal component tends to be very small but non-zero across all datasets.

Chapter 3

Partial-Wave Analysis

3.1 Amplitude Formalism

Now we embark on the topic of amplitudes. We wish to describe the dynamics of our reaction in a way that allows us to extract quantum numbers like spin from our data. There are several difficulties in doing so: First, we are trying to determine the properties of many particles at once, and we know that many resonances in this channel overlap in mass space. This precludes the use of a simple Breit-Wigner description of most of these resonances, as overlapping Breit-Wigners do not preserve unitarityTODO: citation. Second, the GlueX experiment uses a linearly polarized photon beam, so it behooves us to use a formalism which can include this polarization. Finally, there are many resonances in this channel, and while we have the largest photoproduction dataset to date, we are still relatively data limited, which further complicates any dynamical description.

Single-Particle Helicity States

We begin by defining a set of observables which are independent of frames and rotations on those frames. This is known as the helicity formalism, where helicity resembles the spin projection along the axis of a particle's motion. First, we define a rotation $R(\alpha, \omega, \gamma)$ as a matrix whose action on a vector is a rotation about the Euler angles α, ω, and γ. For each rotation, we can define a unitary operator $U[R]$ which has the group property $U[R_2 R_1] = U[R_2]U[R_1]$ as it is an operator on the group $SO(3)$. Being an operator on $SO(3)$, we can also write it as

$$U[R(\alpha, \omega, \gamma)] = e^{-\imath \alpha J_z} e^{-\imath \omega J_y} e^{-\imath \gamma J_z} \tag{3.1}$$

27

We can then describe the matrix elements of this operator in the angular momentum eigenbasis $|jm\rangle$ (representing a spin-j particle where m is the projection of spin onto the $\hat{z}$-axis) with the Wigner D-matrix:

$$U[R(\alpha, \omega, \gamma)] \equiv \sum_{m'} |jm\rangle D^{j}_{m'm}(R(\alpha, \omega, \gamma)) \tag{3.2}$$

where

$$D^{j}_{m'm}(\alpha, \omega, \gamma) \equiv e^{-\imath m' \alpha} d^{j}_{m'm} e^{-\imath m \gamma} \tag{3.3}$$

and

$$d^{j}_{m'm}(\omega) = \left\langle jm' \middle| e^{-\imath \omega J_y} \middle| jm \right\rangle \tag{3.4}$$

We can further extend this eigenbasis to include linear momentum by introducing Lorentz boosts $L(\vec{\beta})$. We denote the operation of a boost along the $\hat{z}$-axis with velocity β as $L_z(\beta)$. A boost in any direction described by polar angles (θ, φ) can be achieved by rotating the $\hat{z}$-axis to align with the direction vector, boosting in the new $\hat{z}$-direction, and rotating back:

$$L(\vec{\beta}) = R(\varphi, \theta, 0)L_z(\beta)R^{-1}(\varphi, \theta, 0) \tag{3.5}$$

Together, the space of rotations and boosts defines the Lorentz group, where each arbitrary Lorentz transformation Λ has a unitary operator $U[\Lambda]$ with the group property $U[\Lambda_2 \Lambda_1] = U[\Lambda_2]U[\Lambda_1]$, so in terms of operators, we can also write

$$U[L(\vec{p})] = U[R(\varphi, \theta, 0)]U[L_z(p)]U^{-1}[R(\varphi, \theta, 0)] \tag{3.6}$$

Finally, this allows us to define the "canonical" basis for a single particle as

$$U[L(\vec{p})]|jm\rangle \equiv |\vec{p}, jm\rangle \tag{3.7}$$

Unfortunately, the quantum number m is only valid in the rest frame of the state because the $\hat{z}$-axis of the rest frame is not equivalent to the $\hat{z}$-axis in any arbitrarily Lorentz-transformed frame. Therefore, we will define helicity λ as the projection of spin along the direction of motion and introduce new helicity states,

$$|\vec{p}, j\lambda\rangle = U[L(\vec{p})]U[R(\varphi, \theta, 0)]|j\lambda\rangle = U[R(\varphi, \theta, 0)]U[L_z(p)]|j\lambda\rangle \tag{3.8}$$

In this definition, we have two ways of obtaining the helicity frame: We can either rotate the state first such that the quantization axis is aligned with $\vec{p}$ and then boost in the $\hat{p}$-direction or we can first boost in the $\hat{z}$-direction and then rotate. In either equivalent case, λ is invariant under rotations as well as boosts parallel to $\vec{p}$. Finally, we can define these helicity states over a basis of canonical states:

$$|\vec{p}, j\lambda\rangle = \sum_m D^j_{m\lambda}(R(\varphi, \theta, 0))\,|\vec{p}, jm\rangle \tag{3.9}$$

The single-particle states are normalized such that

$$\langle \vec{p}', j'\lambda' | \vec{p}, j\lambda \rangle = \tilde{\delta}(\vec{p}' - \vec{p})\delta_{j'j}\delta_{\lambda'\lambda} \tag{3.10}$$

$$\text{with } \tilde{\delta}(\vec{p}' - \vec{p}) = (2\pi)^3 (2E)\delta^{(3)}(\vec{p}' - \vec{p})$$

since the Lorentz-invariant phase space element is given by $\tilde{d}p = \frac{d^3\vec{p}}{(2\pi)^3(2E)}$. This gives the following representation of the identity:

$$\sum_{j\lambda} \int |\vec{p}, j\lambda\rangle\,\tilde{d}p\,\langle \vec{p}, j\lambda| = I \tag{3.11}$$

Two-Particle Helicity States

Of course, we would like to extend these states to be able to talk about interactions and decays. For notation, I will use Ω to represent the polar angles θ and φ and $\varnothing$ to describe the specific value of 0 for both of these angles. Similarly, R_Ω and $R_\varnothing$ will represent the corresponding rotation operators (the second being a null rotation the direction of the $\hat{z}$-axis). R without subscript or angles will represent an arbitrary rotation whose angles are not important for the derivation.

Next, we can define a joint state of two particles with masses w_1 and w_2 (to avoid confusion with angular moments) and spins s_1 and s_2. In the center-of-momentum (COM) frame, these particles are back-to-back, and we can define the momentum of particle 1 as $\vec{p}$ with direction Ω and particle 2 as $-\vec{p}$. Then the joint canonical state, up to a normalization constant $\mathcal{N}$, is given by

$$|\Omega, s_1m_1s_2m_2\rangle = \mathcal{N}\,U[L(\vec{p})]\,|s_1m_1\rangle\,U[L(-\vec{p})]\,|s_2m_2\rangle \tag{3.12}$$

Such a state can also be described with a total spin s and moment m_s:

$$|\Omega, sm_s\rangle = \sum_{m_1m_2} (s_1m_1s_2m_2 \mid sm_s)\,|\Omega, s_1m_1s_2m_2\rangle \tag{3.13}$$

Here, $(s_1m_1s_2m_2 \mid sm_s)$ is the Clebsch-Gordan coefficient describing the angular momentum coupling. Next, we can add additional angular momentum apart from the spin. For a system with angular momentum ℓ with moment m, we use the fact that $\langle \Omega | \ell m \rangle = Y_\ell^m(\Omega)$ (spherical harmonics) to define

$$|\ell m sm_s\rangle = \int d\Omega\, Y_\ell^m(\Omega)\,|\Omega; sm_s\rangle \tag{3.14}$$

Next, the spin s and angular momentum ℓ can be coupled into the total angular momentum J with moment M:

$$|JM\ell m s m_s\rangle = \sum_{m\, m_s} (\ell m s m_s \mid JM)\,|\ell m s m_s\rangle \tag{3.15}$$

This coupled state is still in the canonical formalism, and we would like to use the helicity basis. Using Equation (3.8),

$$|\Omega, s_1\lambda_1 s_2\lambda_2\rangle = \mathcal{N}\,U[R_\Omega]\underbrace{\left(U[L_z(p)]\,|s_1\lambda_1\rangle\,U[L_{-z}(p)]\,|s_2, -\lambda_2\rangle\right)}_{|\varnothing,\, s_1\lambda_1 s_2\lambda_2\rangle} \tag{3.16}$$

To obtain states with a total angular momentum, we can integrate over the space of all rotations, weighted by Wigner D-matrices:

$$|JM s_1\lambda_1 s_2\lambda_2\rangle = \frac{N_J}{2\pi}\int \mathrm{d}R\, D_{M\mu}^{J*}(R)U[R]\,|\varnothing,\, s_1\lambda_1 s_2\lambda_2\rangle \tag{3.17}$$

This is, of course, incomplete, as we have not defined the normalization factor N_J or the coupling μ which relates helicities to total angular momentum. To do both, let us specify the rotation R as follows,

$$\begin{aligned}
|JM s_1\lambda_1 s_2\lambda_2\rangle &= \frac{N_J}{2\pi}\int \mathrm{d}R\, D_{M\mu}^{J*}(R)U[R(\varphi, \theta, \gamma)]\,|\varnothing,\, s_1\lambda_1 s_2\lambda_2\rangle \\
&= \frac{N_J}{2\pi}\int \mathrm{d}R\, D_{M\mu}^{J*}(R)U[R(\varphi, \theta, 0)]U[R(0, 0, \gamma)]\,|\varnothing,\, s_1\lambda_1 s_2\lambda_2\rangle \\
&= \frac{N_J}{2\pi}\int \mathrm{d}R\, D_{M\mu}^{J*}(R)e^{-\imath(\lambda_1-\lambda_2)\gamma}U[R(\varphi, \theta, 0)]\,|\varnothing,\, s_1\lambda_1 s_2\lambda_2\rangle \\
&= \frac{N_J}{2\pi}\int \mathrm{d}\Omega\,\mathrm{d}\gamma\, e^{\imath M\varphi} d_{M\mu}^{J*}e^{\imath\mu\gamma}e^{-\imath(\lambda_1-\lambda_2)\gamma}U[R(\varphi, \theta, 0)]\,|\varnothing,\, s_1\lambda_1 s_2\lambda_2\rangle \\
&= \frac{N_J}{2\pi}\int \mathrm{d}\Omega\,\mathrm{d}\gamma\, e^{\imath M\varphi} d_{M\mu}^{J*}e^{\imath(\mu-(\lambda_1-\lambda_2))\gamma}\,|\Omega,\, s_1\lambda_1 s_2\lambda_2\rangle \\
&= N_J\int \mathrm{d}\Omega\, D_{M\lambda}^{J*}(R_\Omega)\,|\Omega,\, s_1\lambda_1 s_2\lambda_2\rangle \tag{3.18}
\end{aligned}$$

with $\lambda = \lambda_1 - \lambda_2$

It can be shown that the normalization $\mathcal{N} = \frac{1}{4\pi}\sqrt{\frac{p}{w}}$ where p is the relative momentum and w the effective mass of the two-particle system. The normalization of the standard two-particle states is given by

$$\langle \Omega', s_1'\lambda_1' s_2'\lambda_2' | \Omega, s_1\lambda_1 s_2\lambda_2\rangle = \delta^{(2)}(\Omega' - \Omega)\delta_{s_1' s_1}\delta_{\lambda_1'\lambda_1}\delta_{s_2' s_2}\delta_{\lambda_2'\lambda_2} \tag{3.19}$$

This follows immediately from Section 3.1. Next, to ensure that

$$\langle J'M' s_1'\lambda_1' s_2'\lambda_2' | JM s_1\lambda_1 s_2\lambda_2\rangle = \delta_{J'J}\delta_{M'M}\delta_{s_1' s_1}\delta_{\lambda_1'\lambda_1}\delta_{s_2' s_2}\delta_{\lambda_2'\lambda_2} \tag{3.20}$$

we must have $N_J = \sqrt{\frac{2J+1}{4\pi}}$. Finally,

$$\left\langle \Omega, s_1'\lambda_1's_2'\lambda_2' \middle| JMs_1\lambda_1s_2\lambda_2 \right\rangle = N_J D_{M\lambda}^{J*}(R_\Omega)\delta_{s_1's_1}\delta_{\lambda_1'\lambda_1}\delta_{s_2's_2}\delta_{\lambda_2'\lambda_2} \tag{3.21}$$

Production Amplitudes

TODO: cite https://link.springer.com/article/10.1140/epjc/s10052-020-7930-x

Including Linear Polarization

3.2 The Z_ℓ^m Amplitude

3.3 The K-Matrix Parameterization

3.4 Waveset Selection

Chapter 4

Results and Systematic Studies

4.1   Mass-Independent Fits

4.2   Mass-Dependent Fits

4.3   Systematics

Chapter 5

Conclusion

Appendix A

Derivation of the Chew-Mandelstam Function

We begin with the dispersion integral[1]:

$$C(s) = C(s_{\text{thr}}) - \frac{s - s_{\text{thr}}}{\pi} \int_{s_{\text{thr}}}^{\infty} ds' \, \frac{\rho(s')}{(s' - s)(s' - s_{\text{thr}})} \tag{A.1}$$

where $s_{\text{thr}} = (m_1 + m_2)^2$ and

$$\rho(s) = \sqrt{\left(1 - \frac{(m_1 + m_2)^2}{s}\right)\left(1 - \frac{(m_1 - m_2)^2}{s}\right)} \tag{A.2}$$

We first focus on just the integral part:

$$I(s) = \int_{s_{\text{thr}}}^{\infty} ds' \, \frac{\rho(s')}{(s' - s)(s' - s_{\text{thr}})} \tag{A.3}$$

$$\lim_{\epsilon \to 0} \int_{a}^{b} dx \, \frac{f(x)}{(x - x_0) + \iota\epsilon} = \fint_{a}^{b} dx \, \frac{f(x)}{(x - x_0)} + \iota\pi f(x_0) \tag{A.4}$$

$$I(s) = \fint_{s_{\text{thr}}}^{\infty} \tag{A.5}$$

---

[1] see arXiv paper

37

Bibliography

[1] Aristotle, *Metaphysics*. 1.4,985b10-15. type: classic.

[2] Aristotle, *Physics*. 6.1-3,231a21-234b10.

[3] J. Dalton, *A New System of Chemical Philosophy*. Manchester: Printed by S. Russell for R. Bickerstaff, Strand, London.

[4] J. J. Thomson, "Cathode rays," vol. 44, pp. 293–316.

[5] J. J. Thomson, *The Corpuscular Theory of Matter*. Scribner's Sons, New York.

[6] E. Rutherford, "LXXIX. the scattering of α and β particles by matter and the structure of the atom," vol. 21, no. 125, pp. 669–688. Publisher: Taylor & Francis _eprint: https://doi.org/10.1080/14786440508637080.

[7] O. Masson, "XXIV. the constitution of atoms," vol. 41, no. 242, pp. 281–285. Publisher: Taylor & Francis _eprint: https://doi.org/10.1080/14786442108636219.

[8] J. Chadwick, "Possible existence of a neutron," vol. 129, no. 3252, pp. 312–312. Publisher: Nature Publishing Group.

[9] M. Gell-Mann, "A schematic model of baryons and mesons," vol. 8, no. 3, pp. 214–215.

[10] G. Aad, T. Abajyan, B. Abbott, J. Abdallah, S. Abdel Khalek, A. A. Abdelalim, O. Abdinov, R. Aben, B. Abi, M. Abolins, O. S. AbouZeid, H. Abramowicz, H. Abreu, B. S. Acharya, L. Adamczyk, D. L. Adams, T. N. Addy, J. Adelman, S. Adomeit, P. Adragna, T. Adye, S. Aefsky, J. A. Aguilar-Saavedra, M. Agustoni, M. Aharrouche, S. P. Ahlen, F. Ahles, A. Ahmad, M. Ahsan, G. Aielli, T. Akdogan, T. P. A. Åkesson, G. Akimoto, A. V. Akimov, M. S. Alam, M. A. Alam, J. Albert, S. Albrand, M. Aleksa, I. N. Aleksandrov, F. Alessandria, C. Alexa, G. Alexander, G. Alexandre, T. Alexopoulos, M. Alhroob, M. Aliev, G. Alimonti, J. Alison, B. M. M. Allbrooke, P. P. Allport, S. E. Allwood-Spiers, J. Almond, A. Aloisio, R. Alon, A. Alonso, F. Alonso, A. Altheimer, B. Alvarez Gonzalez, M. G. Alviggi, K. Amako, C. Amelung, V. V. Ammosov, S. P. Amor Dos Santos, A. Amorim, N. Amram, C. Anastopoulos, L. S. Ancu, N. Andari, T. Andeen, C. F. Anders, G. Anders, K. J. Anderson, A. Andreazza,

V. Andrei, M. L. Andrieux, X. S. Anduaga, S. Angelidakis, P. Anger, A. Angerami, F. Anghinolfi, A. Anisenkov, N. Anjos, A. Annovi, A. Antonaki, M. Antonelli, A. Antonov, J. Antos, F. Anulli, M. Aoki, S. Aoun, L. Aperio Bella, R. Apolle, G. Arabidze, I. Aracena, Y. Arai, A. T. H. Arce, S. Arfaoui, J. F. Arguin, E. Arik, M. Arik, A. J. Armbruster, O. Arnaez, V. Arnal, C. Arnault, A. Artamonov, G. Artoni, D. Arutinov, S. Asai, S. Ask, B. Åsman, L. Asquith, K. Assamagan, A. Astbury, M. Atkinson, B. Aubert, E. Auge, K. Augsten, M. Aurousseau, G. Avolio, R. Avramidou, D. Axen, G. Azuelos, Y. Azuma, M. A. Baak, G. Baccaglioni, C. Bacci, A. M. Bach, H. Bachacou, K. Bachas, M. Backes, M. Backhaus, J. Backus Mayes, E. Badescu, P. Bagnaia, S. Bahinipati, Y. Bai, D. C. Bailey, T. Bain, J. T. Baines, O. K. Baker, M. D. Baker, S. Baker, P. Balek, E. Banas, P. Banerjee, S. Banerjee, D. Banfi, A. Bangert, V. Bansal, H. S. Bansil, L. Barak, S. P. Baranov, A. Barbaro Galtieri, T. Barber, E. L. Barberio, D. Barberis, M. Barbero, D. Y. Bardin, T. Barillari, M. Barisonzi, T. Barklow, N. Barlow, B. M. Barnett, R. M. Barnett, A. Baroncelli, G. Barone, A. J. Barr, F. Barreiro, J. Barreiro Guimarães da Costa, P. Barrillon, R. Bartoldus, A. E. Barton, V. Bartsch, A. Basye, R. L. Bates, L. Batkova, J. R. Batley, A. Battaglia, M. Battistin, F. Bauer, H. S. Bawa, S. Beale, T. Beau, P. H. Beauchemin, R. Beccherle, P. Bechtle, H. P. Beck, A. K. Becker, S. Becker, M. Beckingham, K. H. Becks, A. J. Beddall, A. Beddall, S. Bedikian, V. A. Bednyakov, C. P. Bee, L. J. Beemster, M. Begel, S. Behar Harpaz, P. K. Behera, M. Beimforde, C. Belanger-Champagne, P. J. Bell, W. H. Bell, G. Bella, L. Bellagamba, M. Bellomo, A. Belloni, O. Beloborodova, K. Belotskiy, O. Beltramello, O. Benary, D. Benchekroun, K. Bendtz, N. Benekos, Y. Benhammou, E. Benhar Noccioli, J. A. Benitez Garcia, D. P. Benjamin, M. Benoit, J. R. Bensinger, K. Benslama, S. Bentvelsen, D. Berge, E. Bergeaas Kuutmann, N. Berger, F. Berghaus, E. Berglund, J. Beringer, P. Bernat, R. Bernhard, C. Bernius, F. U. Bernlochner, T. Berry, C. Bertella, A. Bertin, F. Bertolucci, M. I. Besana, G. J. Besjes, N. Besson, S. Bethke, W. Bhimji, R. M. Bianchi, M. Bianco, O. Biebel, S. P. Bieniek, K. Bierwagen, J. Biesiada, M. Biglietti, H. Bilokon, M. Bindi, S. Binet, A. Bingul, C. Bini, C. Biscarat, B. Bittner, K. M. Black, R. E. Blair, J. B. Blanchard, G. Blanchot, T. Blazek, I. Bloch, C. Blocker, J. Blocki, A. Blondel, W. Blum, U. Blumenschein, G. J. Bobbink, V. B. Bobrovnikov, S. S. Bocchetta, A. Bocci, C. R. Boddy, M. Boehler, J. Boek, N. Boelaert, J. A. Bogaerts, A. Bogdanchikov, A. Bogouch, C. Bohm, J. Bohm, V. Boisvert, T. Bold, V. Boldea, N. M. Bolnet, M. Bomben, M. Bona, M. Boonekamp, S. Bordoni, C. Borer, A. Borisov, G. Borissov, I. Borjanovic, M. Borri, S. Borroni, V. Bortolotto, K. Bos, D. Boscherini, M. Bosman, H. Boterenbrood, J. Bouchami, J. Boudreau, E. V. Bouhova-Thacker, D. Boumediene, C. Bourdarios, N. Bousson, A. Boveia, J. Boyd, I. R. Boyko, I. Bozovic-Jelisavcic, J. Bracinik, P. Branchini, G. W. Brandenburg, A. Brandt, G. Brandt, O. Brandt, U. Bratzler, B. Brau, J. E. Brau, H. M. Braun, S. F. Brazzale, B. Brelier, J. Bremer, K. Brendlinger, R. Brenner, S. Bressler, D. Britton, F. M. Brochu, I. Brock, R. Brock, F. Broggi, C. Bromberg, J. Bronner, G. Brooijmans, T. Brooks, W. K. Brooks, G. Brown, H. Brown, P. A. Bruckman de Renstrom, D. Bruncko, R. Bruneliere, S. Brunet, A. Bruni, G. Bruni, M. Bruschi, T. Buanes, Q. Buat, F. Bucci, J. Buchanan, P. Buchholz, R. M. Buckingham, A. G. Buckley, S. I. Buda, I. A. Budagov, B. Budick, V. Büscher, L. Bugge, O. Bulekov, A. C. Bundock, M. Bunse, T. Buran, H. Burckhart,

S. Burdin, T. Burgess, S. Burke, E. Busato, P. Bussey, C. P. Buszello, B. Butler, J. M. Butler, C. M. Buttar, J. M. Butterworth, W. Buttinger, S. Cabrera Urbán, D. Caforio, O. Cakir, P. Calafiura, G. Calderini, P. Calfayan, R. Calkins, L. P. Caloba, R. Caloi, D. Calvet, S. Calvet, R. Camacho Toro, P. Camarri, D. Cameron, L. M. Caminada, R. Caminal Armadans, S. Campana, M. Campanelli, V. Canale, F. Canelli, A. Canepa, J. Cantero, R. Cantrill, L. Capasso, M. D. M. Capeans Garrido, I. Caprini, M. Caprini, D. Capriotti, M. Capua, R. Caputo, R. Cardarelli, T. Carli, G. Carlino, L. Carminati, B. Caron, S. Caron, E. Carquin, G. D. Carrillo-Montoya, A. A. Carter, J. R. Carter, J. Carvalho, D. Casadei, M. P. Casado, M. Cascella, C. Caso, A. M. Castaneda Hernandez, E. Castaneda-Miranda, V. Castillo Gimenez, N. F. Castro, G. Cataldi, P. Catastini, A. Catinaccio, J. R. Catmore, A. Cattai, G. Cattani, S. Caughron, V. Cavaliere, P. Cavalleri, D. Cavalli, M. Cavalli-Sforza, V. Cavasinni, F. Ceradini, A. S. Cerqueira, A. Cerri, L. Cerrito, F. Cerutti, S. A. Cetin, A. Chafaq, D. Chakraborty, I. Chalupkova, K. Chan, P. Chang, B. Chapleau, J. D. Chapman, J. W. Chapman, E. Chareyre, D. G. Charlton, V. Chavda, C. A. Chavez Barajas, S. Cheatham, S. Chekanov, S. V. Chekulaev, G. A. Chelkov, M. A. Chelstowska, C. Chen, H. Chen, S. Chen, X. Chen, Y. Chen, Y. Cheng, A. Cheplakov, R. Cherkaoui El Moursli, V. Chernyatin, E. Cheu, S. L. Cheung, L. Chevalier, G. Chiefari, L. Chikovani, J. T. Childers, A. Chilingarov, G. Chiodini, A. S. Chisholm, R. T. Chislett, A. Chitan, M. V. Chizhov, G. Choudalakis, S. Chouridou, I. A. Christidi, A. Christov, D. Chromek-Burckhart, M. L. Chu, J. Chudoba, G. Ciapetti, A. K. Ciftci, R. Ciftci, D. Cinca, V. Cindro, C. Ciocca, A. Ciocio, M. Cirilli, P. Cirkovic, Z. H. Citron, M. Citterio, M. Ciubancan, A. Clark, P. J. Clark, R. N. Clarke, W. Cleland, J. C. Clemens, B. Clement, C. Clement, Y. Coadou, M. Cobal, A. Coccaro, J. Cochran, L. Coffey, J. G. Cogan, J. Coggeshall, E. Cogneras, J. Colas, S. Cole, A. P. Colijn, N. J. Collins, C. Collins-Tooth, J. Collot, T. Colombo, G. Colon, G. Compostella, P. Conde Muiño, E. Coniavitis, M. C. Conidi, S. M. Consonni, V. Consorti, S. Constantinescu, C. Conta, G. Conti, F. Conventi, M. Cooke, B. D. Cooper, A. M. Cooper-Sarkar, N. J. Cooper-Smith, K. Copic, T. Cornelissen, M. Corradi, F. Corriveau, A. Cortes-Gonzalez, G. Cortiana, G. Costa, M. J. Costa, D. Costanzo, D. Côté, L. Courneyea, G. Cowan, C. Cowden, B. E. Cox, K. Cranmer, F. Crescioli, M. Cristinziani, G. Crosetti, S. Crépé-Renaudin, C. M. Cuciuc, C. Cuenca Almenar, T. Cuhadar Donszelmann, M. Curatolo, C. J. Curtis, C. Cuthbert, P. Cwetanski, H. Czirr, P. Czodrowski, Z. Czyczula, S. DAuria, M. DOnofrio, A. DOrazio, M. J. Da Cunha Sargedas De Sousa, C. Da Via, W. Dabrowski, A. Dafinca, T. Dai, C. Dallapiccola, M. Dam, M. Dameri, D. S. Damiani, H. O. Danielsson, V. Dao, G. Darbo, G. L. Darlea, J. A. Dassoulas, W. Davey, T. Davidek, N. Davidson, R. Davidson, E. Davies, M. Davies, O. Davignon, A. R. Davison, Y. Davygora, E. Dawe, I. Dawson, R. K. Daya-Ishmukhametova, K. De, R. de Asmundis, S. De Castro, S. De Cecco, J. de Graat, N. De Groot, P. de Jong, C. De La Taille, H. De la Torre, F. De Lorenzi, L. de Mora, L. De Nooij, D. De Pedis, A. De Salvo, U. De Sanctis, A. De Santo, J. B. De Vivie De Regie, G. De Zorzi, W. J. Dearnaley, R. Debbe, C. Debenedetti, B. Dechenaux, D. V. Dedovich, J. Degenhardt, C. Del Papa, J. Del Peso, T. Del Prete, T. Delemontex, M. Deliyergiyev, A. DellAcqua, L. DellAsta, M. Della Pietra, D. della Volpe, M. Delmastro, P. Delpierre, P. A. Delsart, C. Deluca, S. Demers, M. Demichev, B. Demirkoz,

J. Deng, S. P. Denisov, D. Derendarz, J. E. Derkaoui, F. Derue, P. Dervan, K. Desch, E. Devetak, P. O. Deviveiros, A. Dewhurst, B. DeWilde, S. Dhaliwal, R. Dhullipudi, A. Di Ciaccio, L. Di Ciaccio, C. Di Donato, A. Di Girolamo, B. Di Girolamo, S. Di Luise, A. Di Mattia, B. Di Micco, R. Di Nardo, A. Di Simone, R. Di Sipio, M. A. Diaz, E. B. Diehl, J. Dietrich, T. A. Dietzsch, S. Diglio, K. Dindar Yagci, J. Dingfelder, F. Dinut, C. Dionisi, P. Dita, S. Dita, F. Dittus, F. Djama, T. Djobava, M. A. B. do Vale, A. Do Valle Wemans, T. K. O. Doan, M. Dobbs, R. Dobinson, D. Dobos, E. Dobson, J. Dodd, C. Doglioni, T. Doherty, Y. Doi, J. Dolejsi, I. Dolenc, Z. Dolezal, B. A. Dolgoshein, T. Dohmae, M. Donadelli, J. Donini, J. Dopke, A. Doria, A. Dos Anjos, A. Dotti, M. T. Dova, J. D. Dowell, A. D. Doxiadis, A. T. Doyle, N. Dressnandt, M. Dris, J. Dubbert, S. Dube, E. Duchovni, G. Duckeck, D. Duda, A. Dudarev, F. Dudziak, M. Dührssen, I. P. Duerdoth, L. Duflot, M. A. Dufour, L. Duguid, M. Dunford, H. Duran Yildiz, R. Duxfield, M. Dwuznik, F. Dydak, M. Düren, W. L. Ebenstein, J. Ebke, S. Eckweiler, K. Edmonds, W. Edson, C. A. Edwards, N. C. Edwards, W. Ehrenfeld, T. Eifert, G. Eigen, K. Einsweiler, E. Eisenhandler, T. Ekelof, M. El Kacimi, M. Ellert, S. Elles, F. Ellinghaus, K. Ellis, N. Ellis, J. Elmsheuser, M. Elsing, D. Emeliyanov, R. Engelmann, A. Engl, B. Epp, J. Erdmann, A. Ereditato, D. Eriksson, J. Ernst, M. Ernst, J. Ernwein, D. Errede, S. Errede, E. Ertel, M. Escalier, H. Esch, C. Escobar, X. Espinal Curull, B. Esposito, F. Etienne, A. I. Etienvre, E. Etzion, D. Evangelakou, H. Evans, L. Fabbri, C. Fabre, R. M. Fakhrutdinov, S. Falciano, Y. Fang, M. Fanti, A. Farbin, A. Farilla, J. Farley, T. Farooque, S. Farrell, S. M. Farrington, P. Farthouat, F. Fassi, P. Fassnacht, D. Fassouliotis, B. Fatholahzadeh, A. Favareto, L. Fayard, S. Fazio, R. Febbraro, P. Federic, O. L. Fedin, W. Fedorko, M. Fehling-Kaschek, L. Feligioni, D. Fellmann, C. Feng, E. J. Feng, A. B. Fenyuk, J. Ferencei, W. Fernando, S. Ferrag, J. Ferrando, V. Ferrara, A. Ferrari, P. Ferrari, R. Ferrari, D. E. Ferreira de Lima, A. Ferrer, D. Ferrere, C. Ferretti, A. Ferretto Parodi, M. Fiascaris, F. Fiedler, A. Filipčič, F. Filthaut, M. Fincke-Keeler, M. C. N. Fiolhais, L. Fiorini, A. Firan, G. Fischer, M. J. Fisher, M. Flechl, I. Fleck, J. Fleckner, P. Fleischmann, S. Fleischmann, T. Flick, A. Floderus, L. R. Flores Castillo, M. J. Flowerdew, T. Fonseca Martin, A. Formica, A. Forti, D. Fortin, D. Fournier, A. J. Fowler, H. Fox, P. Francavilla, M. Franchini, S. Franchino, D. Francis, T. Frank, M. Franklin, S. Franz, M. Fraternali, S. Fratina, S. T. French, C. Friedrich, F. Friedrich, R. Froeschl, D. Froidevaux, J. A. Frost, C. Fukunaga, E. Fullana Torregrosa, B. G. Fulsom, J. Fuster, C. Gabaldon, O. Gabizon, S. Gadatsch, T. Gadfort, S. Gadomski, G. Gagliardi, P. Gagnon, C. Galea, B. Galhardo, E. J. Gallas, V. Gallo, B. J. Gallop, P. Gallus, K. K. Gan, Y. S. Gao, A. Gaponenko, F. Garberson, M. Garcia-Sciveres, C. García, J. E. García Navarro, R. W. Gardner, N. Garelli, H. Garitaonandia, V. Garonne, C. Gatti, G. Gaudio, B. Gaur, L. Gauthier, P. Gauzzi, I. L. Gavrilenko, C. Gay, G. Gaycken, E. N. Gazis, P. Ge, Z. Gecse, C. N. P. Gee, D. A. A. Geerts, C. Geich-Gimbel, K. Gellerstedt, C. Gemme, A. Gemmell, M. H. Genest, S. Gentile, M. George, S. George, P. Gerlach, A. Gershon, C. Geweniger, H. Ghazlane, N. Ghodbane, B. Giacobbe, S. Giagu, V. Giakoumopoulou, V. Giangiobbe, F. Gianotti, B. Gibbard, A. Gibson, S. M. Gibson, M. Gilchriese, O. Gildemeister, D. Gillberg, A. R. Gillman, D. M. Gingrich, J. Ginzburg, N. Giokaris, M. P. Giordani, R. Giordano, F. M. Giorgi, P. Giovannini, P. F. Giraud, D. Giugni, M. Giunta, P. Giusti, B. K. Gjelsten, L. K. Gladilin,

C. Glasman, J. Glatzer, A. Glazov, K. W. Glitza, G. L. Glonti, J. R. Goddard, J. Godfrey, J. Godlewski, M. Goebel, T. Göpfert, C. Goeringer, C. Gössling, S. Goldfarb, T. Golling, A. Gomes, L. S. Gomez Fajardo, R. Gonçalo, J. Goncalves Pinto Firmino Da Costa, L. Gonella, S. González de la Hoz, G. Gonzalez Parra, M. L. Gonzalez Silva, S. Gonzalez-Sevilla, J. J. Goodson, L. Goossens, P. A. Gorbounov, H. A. Gordon, I. Gorelov, G. Gorfine, B. Gorini, E. Gorini, A. Gorišek, E. Gornicki, B. Gosdzik, A. T. Goshaw, M. Gosselink, M. I. Gostkin, I. Gough Eschrich, M. Gouighri, D. Goujdami, M. P. Goulette, A. G. Goussiou, C. Goy, S. Gozpinar, I. Grabowska-Bold, P. Grafström, K. J. Grahn, E. Gramstad, F. Grancagnolo, S. Grancagnolo, V. Grassi, V. Gratchev, N. Grau, H. M. Gray, J. A. Gray, E. Graziani, O. G. Grebenyuk, T. Greenshaw, Z. D. Greenwood, K. Gregersen, I. M. Gregor, P. Grenier, J. Griffiths, N. Grigalashvili, A. A. Grillo, S. Grinstein, P. Gris, Y. V. Grishkevich, J. F. Grivaz, E. Gross, J. Grosse-Knetter, J. Groth-Jensen, K. Grybel, D. Guest, C. Guicheney, T. Guillemin, S. Guindon, U. Gul, J. Gunther, B. Guo, J. Guo, P. Gutierrez, N. Guttman, O. Gutzwiller, C. Guyot, C. Gwenlan, C. B. Gwilliam, A. Haas, S. Haas, C. Haber, H. K. Hadavand, D. R. Hadley, P. Haefner, F. Hahn, S. Haider, Z. Hajduk, H. Hakobyan, D. Hall, J. Haller, K. Hamacher, P. Hamal, K. Hamano, M. Hamer, A. Hamilton, S. Hamilton, L. Han, K. Hanagaki, K. Hanawa, M. Hance, C. Handel, P. Hanke, J. R. Hansen, J. B. Hansen, J. D. Hansen, P. H. Hansen, P. Hansson, K. Hara, A. S. Hard, G. A. Hare, T. Harenberg, S. Harkusha, D. Harper, R. D. Harrington, O. M. Harris, J. Hartert, F. Hartjes, T. Haruyama, A. Harvey, S. Hasegawa, Y. Hasegawa, S. Hassani, S. Haug, M. Hauschild, R. Hauser, M. Havranek, C. M. Hawkes, R. J. Hawkings, A. D. Hawkins, T. Hayakawa, T. Hayashi, D. Hayden, C. P. Hays, H. S. Hayward, S. J. Haywood, S. J. Head, V. Hedberg, L. Heelan, S. Heim, B. Heinemann, S. Heisterkamp, L. Helary, C. Heller, M. Heller, S. Hellman, D. Hellmich, C. Helsens, R. C. W. Henderson, M. Henke, A. Henrichs, A. M. Henriques Correia, S. Henrot-Versille, C. Hensel, T. Henß, C. M. Hernandez, Y. Hernández Jiménez, R. Herrberg, G. Herten, R. Hertenberger, L. Hervas, G. G. Hesketh, N. P. Hessey, E. Higón-Rodriguez, J. C. Hill, K. H. Hiller, S. Hillert, S. J. Hillier, I. Hinchliffe, E. Hines, M. Hirose, F. Hirsch, D. Hirschbuehl, J. Hobbs, N. Hod, M. C. Hodgkinson, P. Hodgson, A. Hoecker, M. R. Hoeferkamp, J. Hoffman, D. Hoffmann, M. Hohlfeld, M. Holder, S. O. Holmgren, T. Holy, J. L. Holzbauer, T. M. Hong, L. Hooft van Huysduynen, S. Horner, J. Y. Hostachy, S. Hou, A. Hoummada, J. Howard, J. Howarth, I. Hristova, J. Hrivnac, T. Hrynova, P. J. Hsu, S. C. Hsu, D. Hu, Z. Hubacek, F. Hubaut, F. Huegging, A. Huettmann, T. B. Huffman, E. W. Hughes, G. Hughes, M. Huhtinen, M. Hurwitz, N. Huseynov, J. Huston, J. Huth, G. Iacobucci, G. Iakovidis, M. Ibbotson, I. Ibragimov, L. Iconomidou-Fayard, J. Idarraga, P. Iengo, O. Igonkina, Y. Ikegami, M. Ikeno, D. Iliadis, N. Ilic, T. Ince, J. Inigo-Golfin, P. Ioannou, M. Iodice, K. Iordanidou, V. Ippolito, A. Irles Quiles, C. Isaksson, M. Ishino, M. Ishitsuka, R. Ishmukhametov, C. Issever, S. Istin, A. V. Ivashin, W. Iwanski, H. Iwasaki, J. M. Izen, V. Izzo, B. Jackson, J. N. Jackson, P. Jackson, M. R. Jaekel, V. Jain, K. Jakobs, S. Jakobsen, T. Jakoubek, J. Jakubek, D. O. Jamin, D. K. Jana, E. Jansen, H. Jansen, A. Jantsch, M. Janus, G. Jarlskog, L. Jeanty, I. Jen-La Plante, D. Jennens, P. Jenni, A. E. Loevschall-Jensen, P. Jež, S. Jézéquel, M. K. Jha, H. Ji, W. Ji, J. Jia, Y. Jiang, M. Jimenez Belenguer, S. Jin, O. Jinnouchi, M. D. Joergensen, D. Joffe, M. Johansen,

K. E. Johansson, P. Johansson, S. Johnert, K. A. Johns, K. Jon-And, G. Jones, R. W. L. Jones, T. J. Jones, C. Joram, P. M. Jorge, K. D. Joshi, J. Jovicevic, T. Jovin, X. Ju, C. A. Jung, R. M. Jungst, V. Juranek, P. Jussel, A. Juste Rozas, S. Kabana, M. Kaci, A. Kaczmarska, P. Kadlecik, M. Kado, H. Kagan, M. Kagan, E. Kajomovitz, S. Kalinin, L. V. Kalinovskaya, S. Kama, N. Kanaya, M. Kaneda, S. Kaneti, T. Kanno, V. A. Kantserov, J. Kanzaki, B. Kaplan, A. Kapliy, J. Kaplon, D. Kar, M. Karagounis, K. Karakostas, M. Karnevskiy, V. Kartvelishvili, A. N. Karyukhin, L. Kashif, G. Kasieczka, R. D. Kass, A. Kastanas, M. Kataoka, Y. Kataoka, E. Katsoufis, J. Katzy, V. Kaushik, K. Kawagoe, T. Kawamoto, G. Kawamura, M. S. Kayl, S. Kazama, V. A. Kazanin, M. Y. Kazarinov, R. Keeler, P. T. Keener, R. Kehoe, M. Keil, G. D. Kekelidze, J. S. Keller, M. Kenyon, O. Kepka, N. Kerschen, B. P. Kerševan, S. Kersten, K. Kessoku, J. Keung, F. Khalil-zada, H. Khandanyan, A. Khanov, D. Kharchenko, A. Khodinov, A. Khomich, T. J. Khoo, G. Khoriauli, A. Khoroshilov, V. Khovanskiy, E. Khramov, J. Khubua, H. Kim, S. H. Kim, N. Kimura, O. Kind, B. T. King, M. King, R. S. B. King, J. Kirk, A. E. Kiryunin, T. Kishimoto, D. Kisielewska, T. Kitamura, T. Kittelmann, K. Kiuchi, E. Kladiva, M. Klein, U. Klein, K. Kleinknecht, M. Klemetti, A. Klier, P. Klimek, A. Klimentov, R. Klingenberg, J. A. Klinger, E. B. Klinkby, T. Klioutchnikova, P. F. Klok, S. Klous, E. E. Kluge, T. Kluge, P. Kluit, S. Kluth, E. Kneringer, E. B. F. G. Knoops, A. Knue, B. R. Ko, T. Kobayashi, M. Kobel, M. Kocian, P. Kodys, K. Köneke, A. C. König, S. Koenig, L. Köpke, F. Koetsveld, P. Koevesarki, T. Koffas, E. Koffeman, L. A. Kogan, S. Kohlmann, F. Kohn, Z. Kohout, T. Kohriki, T. Koi, G. M. Kolachev, H. Kolanoski, V. Kolesnikov, I. Koletsou, J. Koll, A. A. Komar, Y. Komori, T. Kondo, T. Kono, A. I. Kononov, R. Konoplich, N. Konstantinidis, R. Kopeliansky, S. Koperny, K. Korcyl, K. Kordas, A. Korn, A. Korol, I. Korolkov, E. V. Korolkova, V. A. Korotkov, O. Kortner, S. Kortner, V. V. Kostyukhin, S. Kotov, V. M. Kotov, A. Kotwal, C. Kourkoumelis, V. Kouskoura, A. Koutsman, R. Kowalewski, T. Z. Kowalski, W. Kozanecki, A. S. Kozhin, V. Kral, V. A. Kramarenko, G. Kramberger, M. W. Krasny, A. Krasznahorkay, J. K. Kraus, S. Kreiss, F. Krejci, J. Kretzschmar, N. Krieger, P. Krieger, K. Kroeninger, H. Kroha, J. Kroll, J. Kroseberg, J. Krstic, U. Kruchonak, H. Krüger, T. Kruker, N. Krumnack, Z. V. Krumshteyn, A. Kruse, T. Kubota, S. Kuday, S. Kuehn, A. Kugel, T. Kuhl, D. Kuhn, V. Kukhtin, Y. Kulchitsky, S. Kuleshov, C. Kummer, M. Kuna, J. Kunkle, A. Kupco, H. Kurashige, M. Kurata, Y. A. Kurochkin, V. Kus, E. S. Kuwertz, M. Kuze, J. Kvita, R. Kwee, A. La Rosa, L. La Rotonda, L. Labarga, J. Labbe, S. Lablak, C. Lacasta, F. Lacava, J. Lacey, H. Lacker, D. Lacour, V. R. Lacuesta, E. Ladygin, R. Lafaye, B. Laforge, T. Lagouri, S. Lai, E. Laisne, M. Lamanna, L. Lambourne, C. L. Lampen, W. Lampl, E. Lancon, U. Landgraf, M. P. J. Landon, V. S. Lang, C. Lange, A. J. Lankford, F. Lanni, K. Lantzsch, S. Laplace, C. Lapoire, J. F. Laporte, T. Lari, A. Larner, M. Lassnig, P. Laurelli, V. Lavorini, W. Lavrijsen, P. Laycock, T. Lazovich, O. Le Dortz, E. Le Guirriec, E. Le Menedeu, T. LeCompte, F. Ledroit-Guillon, H. Lee, J. S. H. Lee, S. C. Lee, L. Lee, M. Lefebvre, M. Legendre, F. Legger, C. Leggett, M. Lehmacher, G. Lehmann Miotto, X. Lei, M. A. L. Leite, R. Leitner, D. Lellouch, B. Lemmer, V. Lendermann, K. J. C. Leney, T. Lenz, G. Lenzen, B. Lenzi, K. Leonhardt, S. Leontsinis, F. Lepold, C. Leroy, J. R. Lessard, C. G. Lester, C. M. Lester, J. Levêque, D. Levin, L. J. Levinson, A. Lewis, G. H. Lewis, A. M.

Leyko, M. Leyton, B. Li, H. Li, H. L. Li, S. Li, X. Li, Z. Liang, H. Liao, B. Liberti, P. Lichard, M. Lichtnecker, K. Lie, W. Liebig, C. Limbach, A. Limosani, M. Limper, S. C. Lin, F. Linde, J. T. Linnemann, E. Lipeles, A. Lipniacka, T. M. Liss, D. Lissauer, A. Lister, A. M. Litke, C. Liu, D. Liu, H. Liu, J. B. Liu, K. Liu, L. Liu, M. Liu, Y. Liu, M. Livan, S. S. A. Livermore, A. Lleres, J. Llorente Merino, S. L. Lloyd, E. Lobodzinska, P. Loch, W. S. Lockman, T. Loddenkoetter, F. K. Loebinger, A. Loginov, C. W. Loh, T. Lohse, K. Lohwasser, M. Lokajicek, V. P. Lombardo, J. D. Long, R. E. Long, L. Lopes, D. Lopez Mateos, J. Lorenz, N. Lorenzo Martinez, M. Losada, P. Loscutoff, F. Lo Sterzo, M. J. Losty, X. Lou, A. Lounis, K. F. Loureiro, J. Love, P. A. Love, A. J. Lowe, F. Lu, H. J. Lubatti, C. Luci, A. Lucotte, A. Ludwig, D. Ludwig, I. Ludwig, J. Ludwig, F. Luehring, G. Luijckx, W. Lukas, L. Luminari, E. Lund, B. Lund-Jensen, B. Lundberg, J. Lundberg, O. Lundberg, J. Lundquist, M. Lungwitz, D. Lynn, E. Lytken, H. Ma, L. L. Ma, G. Maccarrone, A. Macchiolo, B. Maček, J. Machado Miguens, R. Mackeprang, R. J. Madaras, H. J. Maddocks, W. F. Mader, R. Maenner, T. Maeno, P. Mättig, S. Mättig, L. Magnoni, E. Magradze, K. Mahboubi, J. Mahlstedt, S. Mahmoud, G. Mahout, C. Maiani, C. Maidantchik, A. Maio, S. Majewski, Y. Makida, N. Makovec, P. Mal, B. Malaescu, P. Malecki, P. Malecki, V. P. Maleev, F. Malek, U. Mallik, D. Malon, C. Malone, S. Maltezos, V. Malyshev, S. Malyukov, R. Mameghani, J. Mamuzic, A. Manabe, L. Mandelli, I. Mandić, R. Mandrysch, J. Maneira, A. Manfredini, P. S. Mangeard, L. Manhaes de Andrade Filho, J. A. Manjarres Ramos, A. Mann, P. M. Manning, A. Manousakis-Katsikakis, B. Mansoulie, A. Mapelli, L. Mapelli, L. March, J. F. Marchand, F. Marchese, G. Marchiori, M. Marcisovsky, C. P. Marino, F. Marroquim, Z. Marshall, F. K. Martens, L. F. Marti, S. Marti-Garcia, B. Martin, B. Martin, J. P. Martin, T. A. Martin, V. J. Martin, B. Martin dit Latour, S. Martin-Haugh, M. Martinez, V. Martinez Outschoorn, A. C. Martyniuk, M. Marx, F. Marzano, A. Marzin, L. Masetti, T. Mashimo, R. Mashinistov, J. Masik, A. L. Maslennikov, I. Massa, G. Massaro, N. Massol, P. Mastrandrea, A. Mastroberardino, T. Masubuchi, P. Matricon, H. Matsunaga, T. Matsushita, C. Mattravers, J. Maurer, S. J. Maxfield, A. Mayne, R. Mazini, M. Mazur, L. Mazzaferro, M. Mazzanti, J. Mc Donald, S. P. Mc Kee, A. McCarn, R. L. McCarthy, T. G. McCarthy, N. A. McCubbin, K. W. McFarlane, J. A. Mcfayden, G. Mchedlidze, T. Mclaughlan, S. J. McMahon, R. A. McPherson, A. Meade, J. Mechnich, M. Mechtel, M. Medinnis, R. Meera-Lebbai, T. Meguro, R. Mehdiyev, S. Mehlhase, A. Mehta, K. Meier, B. Meirose, C. Melachrinos, B. R. Mellado Garcia, F. Meloni, L. Mendoza Navas, Z. Meng, A. Mengarelli, S. Menke, E. Meoni, K. M. Mercurio, P. Mermod, L. Merola, C. Meroni, F. S. Merritt, H. Merritt, A. Messina, J. Metcalfe, A. S. Mete, C. Meyer, C. Meyer, J. P. Meyer, J. Meyer, J. Meyer, T. C. Meyer, S. Michal, L. Micu, R. P. Middleton, S. Migas, L. Mijović, G. Mikenberg, M. Mikestikova, M. Mikuž, D. W. Miller, R. J. Miller, W. J. Mills, C. Mills, A. Milov, D. A. Milstead, D. Milstein, A. A. Minaenko, M. Miñano Moya, I. A. Minashvili, A. I. Mincer, B. Mindur, M. Mineev, Y. Ming, L. M. Mir, G. Mirabelli, J. Mitrevski, V. A. Mitsou, S. Mitsui, P. S. Miyagawa, J. U. Mjörnmark, T. Moa, V. Moeller, K. Mönig, N. Möser, S. Mohapatra, W. Mohr, R. Moles-Valls, A. Molfetas, J. Monk, E. Monnier, J. Montejo Berlingen, F. Monticelli, S. Monzani, R. W. Moore, G. F. Moorhead, C. Mora Herrera, A. Moraes, N. Morange, J. Morel, G. Morello, D. Moreno, M. Moreno Llácer,

P. Morettini, M. Morgenstern, M. Morii, A. K. Morley, G. Mornacchi, J. D. Morris, L. Morvaj, H. G. Moser, M. Mosidze, J. Moss, R. Mount, E. Mountricha, S. V. Mouraviev, E. J. W. Moyse, F. Mueller, J. Mueller, K. Mueller, T. A. Müller, T. Mueller, D. Muenstermann, Y. Munwes, W. J. Murray, I. Mussche, E. Musto, A. G. Myagkov, M. Myska, O. Nackenhorst, J. Nadal, K. Nagai, R. Nagai, K. Nagano, A. Nagarkar, Y. Nagasaka, M. Nagel, A. M. Nairz, Y. Nakahama, K. Nakamura, T. Nakamura, I. Nakano, G. Nanava, A. Napier, R. Narayan, M. Nash, T. Nattermann, T. Naumann, G. Navarro, H. A. Neal, P. Y. Nechaeva, T. J. Neep, A. Negri, G. Negri, M. Negrini, S. Nektarijevic, A. Nelson, T. K. Nelson, S. Nemecek, P. Nemethy, A. A. Nepomuceno, M. Nessi, M. S. Neubauer, M. Neumann, A. Neusiedl, R. M. Neves, P. Nevski, F. M. Newcomer, P. R. Newman, V. Nguyen Thi Hong, R. B. Nickerson, R. Nicolaidou, B. Nicquevert, F. Niedercorn, J. Nielsen, N. Nikiforou, A. Nikiforov, V. Nikolaenko, I. Nikolic-Audit, K. Nikolics, K. Nikolopoulos, H. Nilsen, P. Nilsson, Y. Ninomiya, A. Nisati, R. Nisius, T. Nobe, L. Nodulman, M. Nomachi, I. Nomidis, S. Norberg, M. Nordberg, P. R. Norton, J. Novakova, M. Nozaki, L. Nozka, I. M. Nugent, A. E. Nuncio-Quiroz, G. Nunes Hanninger, T. Nunnemann, E. Nurse, B. J. OBrien, D. C. ONeil, V. OShea, L. B. Oakes, F. G. Oakham, H. Oberlack, J. Ocariz, A. Ochi, S. Oda, S. Odaka, J. Odier, H. Ogren, A. Oh, S. H. Oh, C. C. Ohm, T. Ohshima, W. Okamura, H. Okawa, Y. Okumura, T. Okuyama, A. Olariu, A. G. Olchevski, S. A. Olivares Pino, M. Oliveira, D. Oliveira Damazio, E. Oliver Garcia, D. Olivito, A. Olszewski, J. Olszowska, A. Onofre, P. U. E. Onyisi, C. J. Oram, M. J. Oreglia, Y. Oren, D. Orestano, N. Orlando, I. Orlov, C. Oropeza Barrera, R. S. Orr, B. Osculati, R. Ospanov, C. Osuna, G. Otero y Garzon, J. P. Ottersbach, M. Ouchrif, E. A. Ouellette, F. Ould-Saada, A. Ouraou, Q. Ouyang, A. Ovcharova, M. Owen, S. Owen, V. E. Ozcan, N. Ozturk, A. Pacheco Pages, C. Padilla Aranda, S. Pagan Griso, E. Paganis, C. Pahl, F. Paige, P. Pais, K. Pajchel, G. Palacino, C. P. Paleari, S. Palestini, D. Pallin, A. Palma, J. D. Palmer, Y. B. Pan, E. Panagiotopoulou, J. G. Panduro Vazquez, P. Pani, N. Panikashvili, S. Panitkin, D. Pantea, A. Papadelis, T. D. Papadopoulou, A. Paramonov, D. Paredes Hernandez, W. Park, M. A. Parker, F. Parodi, J. A. Parsons, U. Parzefall, S. Pashapour, E. Pasqualucci, S. Passaggio, A. Passeri, F. Pastore, F. Pastore, G. Pásztor, S. Pataraia, N. Patel, J. R. Pater, S. Patricelli, T. Pauly, M. Pecsy, S. Pedraza Lopez, M. I. Pedraza Morales, S. V. Peleganchuk, D. Pelikan, H. Peng, B. Penning, A. Penson, J. Penwell, M. Perantoni, K. Perez, T. Perez Cavalcanti, E. Perez Codina, M. T. Pérez García-Estañ, V. Perez Reale, L. Perini, H. Pernegger, R. Perrino, P. Perrodo, V. D. Peshekhonov, K. Peters, B. A. Petersen, J. Petersen, T. C. Petersen, E. Petit, A. Petridis, C. Petridou, E. Petrolo, F. Petrucci, D. Petschull, M. Petteni, R. Pezoa, A. Phan, P. W. Phillips, G. Piacquadio, A. Picazio, E. Piccaro, M. Piccinini, S. M. Piec, R. Piegaia, D. T. Pignotti, J. E. Pilcher, A. D. Pilkington, J. Pina, M. Pinamonti, A. Pinder, J. L. Pinfold, B. Pinto, C. Pizio, M. Plamondon, M. A. Pleier, E. Plotnikova, A. Poblaguev, S. Poddar, F. Podlyski, L. Poggioli, D. Pohl, M. Pohl, G. Polesello, A. Policicchio, R. Polifka, A. Polini, J. Poll, V. Polychronakos, D. Pomeroy, K. Pommès, L. Pontecorvo, B. G. Pope, G. A. Popeneciu, D. S. Popovic, A. Poppleton, X. Portell Bueso, G. E. Pospelov, S. Pospisil, I. N. Potrap, C. J. Potter, C. T. Potter, G. Poulard, J. Poveda, V. Pozdnyakov, R. Prabhu, P. Pralavorio, A. Pranko, S. Prasad,

R. Pravahan, S. Prell, K. Pretzl, D. Price, J. Price, L. E. Price, D. Prieur, M. Primavera, K. Prokofiev, F. Prokoshin, S. Protopopescu, J. Proudfoot, X. Prudent, M. Przybycien, H. Przysiezniak, S. Psoroulas, E. Ptacek, E. Pueschel, J. Purdham, M. Purohit, P. Puzo, Y. Pylypchenko, J. Qian, A. Quadt, D. R. Quarrie, W. B. Quayle, F. Quinonez, M. Raas, S. Raddum, V. Radeka, V. Radescu, P. Radloff, T. Rador, F. Ragusa, G. Rahal, A. M. Rahimi, D. Rahm, S. Rajagopalan, M. Rammensee, M. Rammes, A. S. Randle-Conde, K. Randrianarivony, F. Rauscher, T. C. Rave, M. Raymond, A. L. Read, D. M. Rebuzzi, A. Redelbach, G. Redlinger, R. Reece, K. Reeves, E. Reinherz-Aronis, A. Reinsch, I. Reisinger, C. Rembser, Z. L. Ren, A. Renaud, M. Rescigno, S. Resconi, B. Resende, P. Reznicek, R. Rezvani, R. Richter, E. Richter-Was, M. Ridel, M. Rijpstra, M. Rijssenbeek, A. Rimoldi, L. Rinaldi, R. R. Rios, I. Riu, G. Rivoltella, F. Rizatdinova, E. Rizvi, S. H. Robertson, A. Robichaud-Veronneau, D. Robinson, J. E. M. Robinson, A. Robson, J. G. Rocha de Lima, C. Roda, D. Roda Dos Santos, A. Roe, S. Roe, O. Røhne, S. Rolli, A. Romaniouk, M. Romano, G. Romeo, E. Romero Adam, N. Rompotis, L. Roos, E. Ros, S. Rosati, K. Rosbach, A. Rose, M. Rose, G. A. Rosenbaum, E. I. Rosenberg, P. L. Rosendahl, O. Rosenthal, L. Rosselet, V. Rossetti, E. Rossi, L. P. Rossi, M. Rotaru, I. Roth, J. Rothberg, D. Rousseau, C. R. Royon, A. Rozanov, Y. Rozen, X. Ruan, F. Rubbo, I. Rubinskiy, N. Ruckstuhl, V. I. Rud, C. Rudolph, G. Rudolph, F. Rühr, A. Ruiz-Martinez, L. Rumyant-sev, Z. Rurikova, N. A. Rusakovich, J. P. Rutherfoord, P. Ruzicka, Y. F. Ryabov, M. Rybar, G. Rybkin, N. C. Ryder, A. F. Saavedra, I. Sadeh, H. F. W. Sadrozinski, R. Sadykov, F. Safai Tehrani, H. Sakamoto, G. Salamanna, A. Salamon, M. Saleem, D. Salek, D. Salihagic, A. Salnikov, J. Salt, B. M. Salvachua Ferrando, D. Salvatore, F. Sal-vatore, A. Salvucci, A. Salzburger, D. Sampsonidis, B. H. Samset, A. Sanchez, V. Sanchez Martinez, H. Sandaker, H. G. Sander, M. P. Sanders, M. Sandhoff, T. Sandoval, C. Sandoval, R. Sandstroem, D. P. C. Sankey, A. San-soni, C. Santamarina Rios, C. Santoni, R. Santonico, H. Santos, J. G. Saraiva, T. Sarangi, E. Sarkisyan-Grinbaum, F. Sarri, G. Sartisohn, O. Sasaki, Y. Sasaki, N. Sasao, I. Satsounkevitch, G. Sauvage, E. Sauvan, J. B. Sauvan, P. Savard, V. Savinov, D. O. Savu, L. Sawyer, D. H. Saxon, J. Saxon, C. Sbarra, A. Sbrizzi, D. A. Scannicchio, M. Scarcella, J. Schaarschmidt, P. Schacht, D. Schaefer, U. Schäfer, A. Schaelicke, S. Schaepe, S. Schaetzel, A. C. Schaffer, D. Schaile, R. D. Schamberger, A. G. Schamov, V. Scharf, V. A. Schegelsky, D. Scheirich, M. Scher-nau, M. I. Scherzer, C. Schiavi, J. Schieck, M. Schioppa, S. Schlenker, P. Schmid, E. Schmidt, K. Schmieden, C. Schmitt, S. Schmitt, M. Schmitz, B. Schneider, U. Schnoor, L. Schoeffel, A. Schoening, A. L. S. Schorlemmer, M. Schott, D. Schouten, J. Schovancova, M. Schram, C. Schroeder, N. Schroer, M. J. Schultens, J. Schultes, H. C. Schultz-Coulon, H. Schulz, M. Schumacher, B. A. Schumm, P. Schune, C. Schwanenberger, A. Schwartzman, P. Schwegler, P. Schwemling, R. Schwienhorst, R. Schwierz, J. Schwindling, T. Schwindt, M. Schwoerer, G. Sci-olla, W. G. Scott, J. Searcy, G. Sedov, E. Sedykh, S. C. Seidel, A. Seiden, F. Seifert, J. M. Seixas, G. Sekhniaidze, S. J. Sekula, K. E. Selbach, D. M. Seliverstov, B. Sellden, G. Sellers, M. Seman, N. Semprini-Cesari, C. Serfon, L. Serin, L. Serkin, R. Seuster, H. Severini, A. Sfyrla, E. Shabalina, M. Shamim, L. Y. Shan, J. T. Shank, Q. T. Shao, M. Shapiro, P. B. Shatalov, K. Shaw, D. Sherman, P. Sherwood, S. Shimizu, M. Shimojima, T. Shin, M. Shiyakova,

A. Shmeleva, M. J. Shochet, D. Short, S. Shrestha, E. Shulga, M. A. Shupe, P. Sicho, A. Sidoti, F. Siegert, D. Sijacki, O. Silbert, J. Silva, Y. Silver, D. Silverstein, S. B. Silverstein, V. Simak, O. Simard, L. Simic, S. Simion, E. Simioni, B. Simmons, R. Simoniello, M. Simonyan, P. Sinervo, N. B. Sinev, V. Sipica, G. Siragusa, A. Sircar, A. N. Sisakyan, S. Y. Sivoklokov, J. Sjölin, T. B. Sjursen, L. A. Skinnari, H. P. Skottowe, K. Skovpen, P. Skubic, M. Slater, T. Slav-icek, K. Sliwa, V. Smakhtin, B. H. Smart, L. Smestad, S. Y. Smirnov, Y. Smirnov, L. N. Smirnova, O. Smirnova, B. C. Smith, D. Smith, K. M. Smith, M. Smizanska, K. Smolek, A. A. Snesarev, S. W. Snow, J. Snow, S. Snyder, R. Sobie, J. Sodomka, A. Soffer, C. A. Solans, M. Solar, J. Solc, E. Y. Soldatov, U. Soldevila, E. Solfaroli Camillocci, A. A. Solodkov, O. V. Solovyanov, V. Solovyev, N. Soni, V. Sopko, B. Sopko, M. Sosebee, R. Soualah, A. Soukharev, S. Spagnolo, F. Spanò, W. R. Spearman, R. Spighi, G. Spigo, R. Spiwoks, M. Spousta, T. Spreitzer, B. Spurlock, R. D. St. Denis, J. Stahlman, R. Stamen, E. Stanecka, R. W. Stanek, C. Stanescu, M. Stanescu-Bellu, M. M. Stan-itzki, S. Stapnes, E. A. Starchenko, J. Stark, P. Staroba, P. Starovoitov, R. Staszewski, A. Staude, P. Stavina, G. Steele, P. Steinbach, P. Steinberg, I. Stekl, B. Stelzer, H. J. Stelzer, O. Stelzer-Chilton, H. Stenzel, S. Stern, G. A. Stewart, J. A. Stillings, M. C. Stockton, K. Stoerig, G. Stoicea, S. Stonjek, P. Strachota, A. R. Stradling, A. Straessner, J. Strandberg, S. Strandberg, A. Strandlie, M. Strang, E. Strauss, M. Strauss, P. Strizenec, R. Ströh-mer, D. M. Strom, J. A. Strong, R. Stroynowski, B. Stugu, I. Stumer, J. Stupak, P. Sturm, N. A. Styles, D. A. Soh, D. Su, H. Subramania, R. Subramaniam, A. Succurro, Y. Sugaya, C. Suhr, M. Suk, V. V. Sulin, S. Sultan-soy, T. Sumida, X. Sun, J. E. Sundermann, K. Suruliz, G. Susinno, M. R. Sutton, Y. Suzuki, Y. Suzuki, M. Svatos, S. Swedish, I. Sykora, T. Sykora, J. Sánchez, D. Ta, K. Tackmann, A. Taffard, R. Tafirout, N. Taiblum, Y. Taka-hashi, H. Takai, R. Takashima, H. Takeda, T. Takeshita, Y. Takubo, M. Talby, A. Talyshev, M. C. Tamsett, K. G. Tan, J. Tanaka, R. Tanaka, S. Tanaka, S. Tanaka, A. J. Tanasijczuk, K. Tani, N. Tannoury, S. Tapprogge, D. Tardif, S. Tarem, F. Tarrade, G. F. Tartarelli, P. Tas, M. Tasevsky, E. Tassi, M. Tatarkhanov, Y. Tayalati, C. Taylor, F. E. Taylor, G. N. Taylor, W. Taylor, M. Teinturier, F. A. Teischinger, M. Teixeira Dias Castanheira, P. Teixeira-Dias, K. K. Temming, H. Ten Kate, P. K. Teng, S. Terada, K. Terashi, J. Terron, M. Testa, R. J. Teuscher, J. Therhaag, T. Theveneaux-Pelzer, S. Thoma, J. P. Thomas, E. N. Thompson, P. D. Thompson, P. D. Thompson, A. S. Thomp-son, L. A. Thomsen, E. Thomson, M. Thomson, W. M. Thong, R. P. Thun, F. Tian, M. J. Tibbetts, T. Tic, V. O. Tikhomirov, Y. A. Tikhonov, S. Timoshenko, E. Tiouchichine, P. Tipton, S. Tisserant, T. Todorov, S. Todorova-Nova, B. Toggerson, J. Tojo, S. Tokár, K. Tokushuku, K. Tollefson, M. Tomoto, L. Tompkins, K. Toms, A. Tonoyan, C. Topfel, N. D. Topilin, I. Torchiani, E. Torrence, H. Torres, E. Torró Pastor, J. Toth, F. Touchard, D. R. Tovey, T. Trefzger, L. Tremblet, A. Tricoli, I. M. Trigger, G. Trilling, S. Trincaz-Duvoid, M. F. Tripiana, N. Triplett, W. Trischuk, B. Trocmé, C. Troncon, M. Trottier-McDonald, M. Trzebinski, A. Trzupek, C. Tsarouchas, J. C. L. Tseng, M. Tsiakiris, P. V. Tsiareshka, D. Tsionou, G. Tsipolitis, S. Tsiskaridze, V. Tsiskaridze, E. G. Tskhadadze, I. I. Tsukerman, V. Tsulaia, J. W. Tsung, S. Tsuno, D. Tsybychev, A. Tua, A. Tudorache, V. Tudorache, J. M. Tuggle, M. Turala, D. Turecek, I. Turk Cakir, E. Turlay, R. Turra, P. M. Tuts, A. Tykhonov, M. Tylmad, M. Tyn-

del, G. Tzanakos, K. Uchida, I. Ueda, R. Ueno, M. Ugland, M. Uhlenbrock, M. Uhrmacher, F. Ukegawa, G. Unal, A. Undrus, G. Unel, Y. Unno, D. Urbaniec, P. Urquijo, G. Usai, M. Uslenghi, L. Vacavant, V. Vacek, B. Vachon, S. Vahsen, J. Valenta, S. Valentinetti, A. Valero, S. Valkar, E. Valladolid Gallego, S. Vallecorsa, J. A. Valls Ferrer, R. Van Berg, P. C. Van Der Deijl, R. van der Geer, H. van der Graaf, R. Van Der Leeuw, E. van der Poel, D. van der Ster, N. van Eldik, P. van Gemmeren, I. van Vulpen, M. Vanadia, W. Vandelli, R. Vanguri, A. Vaniachine, P. Vankov, F. Vannucci, R. Vari, T. Varol, D. Varouchas, A. Vartapetian, K. E. Varvell, V. I. Vassilakopoulos, F. Vazeille, T. Vazquez Schroeder, G. Vegni, J. J. Veillet, F. Veloso, R. Veness, S. Veneziano, A. Ventura, D. Ventura, M. Venturi, N. Venturi, V. Vercesi, M. Verducci, W. Verkerke, J. C. Vermeulen, A. Vest, M. C. Vetterli, I. Vichou, T. Vickey, O. E. Vickey Boeriu, G. H. A. Viehhauser, S. Viel, M. Villa, M. Villaplana Perez, E. Vilucchi, M. G. Vincter, E. Vinek, V. B. Vinogradov, M. Virchaux, J. Virzi, O. Vitells, M. Viti, I. Vivarelli, F. Vives Vaque, S. Vlachos, D. Vladoiu, M. Vlasak, A. Vogel, P. Vokac, G. Volpi, M. Volpi, G. Volpini, H. von der Schmitt, H. von Radziewski, E. von Toerne, V. Vorobel, V. Vorwerk, M. Vos, R. Voss, T. T. Voss, J. H. Vossebeld, N. Vranjes, M. Vranjes Milosavljevic, V. Vrba, M. Vreeswijk, T. Vu Anh, R. Vuillermet, I. Vukotic, W. Wagner, P. Wagner, H. Wahlen, S. Wahrmund, J. Wakabayashi, S. Walch, J. Walder, R. Walker, W. Walkowiak, R. Wall, P. Waller, B. Walsh, C. Wang, F. Wang, H. Wang, H. Wang, J. Wang, J. Wang, R. Wang, S. M. Wang, T. Wang, A. Warburton, C. P. Ward, D. R. Wardrope, M. Warsinsky, A. Washbrook, C. Wasicki, I. Watanabe, P. M. Watkins, A. T. Watson, I. J. Watson, M. F. Watson, G. Watts, S. Watts, A. T. Waugh, B. M. Waugh, M. S. Weber, P. Weber, J. S. Webster, A. R. Weidberg, P. Weigell, J. Weingarten, C. Weiser, P. S. Wells, T. Wenaus, D. Wendland, Z. Weng, T. Wengler, S. Wenig, N. Wermes, M. Werner, P. Werner, M. Werth, M. Wessels, J. Wetter, C. Weydert, K. Whalen, S. J. Wheeler-Ellis, A. White, M. J. White, S. White, S. R. Whitehead, D. Whiteson, D. Whittington, F. Wicek, D. Wicke, F. J. Wickens, W. Wiedenmann, M. Wielers, P. Wienemann, C. Wiglesworth, L. A. M. Wiik-Fuchs, P. A. Wijeratne, A. Wildauer, M. A. Wildt, I. Wilhelm, H. G. Wilkens, J. Z. Will, E. Williams, H. H. Williams, W. Willis, S. Willocq, J. A. Wilson, M. G. Wilson, A. Wilson, I. Wingerter-Seez, S. Winkelmann, F. Winklmeier, M. Wittgen, S. J. Wollstadt, M. W. Wolter, H. Wolters, W. C. Wong, G. Wooden, B. K. Wosiek, J. Wotschack, M. J. Woudstra, K. W. Wozniak, K. Wraight, M. Wright, B. Wrona, S. L. Wu, X. Wu, Y. Wu, E. Wulf, B. M. Wynne, S. Xella, M. Xiao, S. Xie, C. Xu, D. Xu, B. Yabsley, S. Yacoob, M. Yamada, H. Yamaguchi, Y. Yamaguchi, A. Yamamoto, K. Yamamoto, S. Yamamoto, T. Yamamura, T. Yamanaka, T. Yamazaki, Y. Yamazaki, Z. Yan, H. Yang, H. Yang, U. K. Yang, Y. Yang, Z. Yang, S. Yanush, L. Yao, Y. Yao, Y. Yasu, G. V. Ybeles Smit, J. Ye, S. Ye, M. Yilmaz, R. Yoosoofmiya, K. Yorita, R. Yoshida, K. Yoshihara, C. Young, C. J. Young, S. Youssef, D. Yu, J. Yu, J. Yu, L. Yuan, A. Yurkewicz, M. Byszewski, B. Zabinski, R. Zaidan, A. M. Zaitsev, Z. Zajacova, L. Zanello, D. Zanzi, A. Zaytsev, C. Zeitnitz, M. Zeman, A. Zemla, C. Zendler, O. Zenin, T. Ženiš, Z. Zinonos, D. Zerwas, G. Zevi della Porta, D. Zhang, H. Zhang, J. Zhang, X. Zhang, Z. Zhang, L. Zhao, Z. Zhao, A. Zhemchugov, J. Zhong, B. Zhou, N. Zhou, Y. Zhou, C. G. Zhu, H. Zhu, J. Zhu, Y. Zhu, X. Zhuang, V. Zhuravlov, D. Zieminska, N. I. Zimin, R. Zimmermann,

S. Zimmermann, S. Zimmermann, M. Ziolkowski, R. Zitoun, L. Živković, V. V. Zmouchko, G. Zobernig, A. Zoccoli, M. zur Nedden, V. Zutshi, and L. Zwalinski, "Observation of a new particle in the search for the standard model higgs boson with the ATLAS detector at the LHC," vol. 716, no. 1, pp. 1–29.

[11] K. G. Wilson, "Confinement of quarks," vol. 10, no. 8, pp. 2445–2459. Publisher: American Physical Society.

[12] C. J. Morningstar and M. Peardon, "Glueball spectrum from an anisotropic lattice study," vol. 60, no. 3, p. 034509.

[13] Particle Data Group, P. A. Zyla, R. M. Barnett, J. Beringer, O. Dahl, D. A. Dwyer, D. E. Groom, C. J. Lin, K. S. Lugovsky, E. Pianori, D. J. Robinson, C. G. Wohl, W. M. Yao, K. Agashe, G. Aielli, B. C. Allanach, C. Amsler, M. Antonelli, E. C. Aschenauer, D. M. Asner, H. Baer, S. Banerjee, L. Baudis, C. W. Bauer, J. J. Beatty, V. I. Belousov, S. Bethke, A. Bettini, O. Biebel, K. M. Black, E. Blucher, O. Buchmuller, V. Burkert, M. A. Bychkov, R. N. Cahn, M. Carena, A. Ceccucci, A. Cerri, D. Chakraborty, R. S. Chivukula, G. Cowan, G. D'Ambrosio, T. Damour, D. De Florian, A. De Gouvêa, T. DeGrand, P. De Jong, G. Dissertori, B. A. Dobrescu, M. D'Onofrio, M. Doser, M. Drees, H. K. Dreiner, P. Eerola, U. Egede, S. Eidelman, J. Ellis, J. Erler, V. V. Ezhela, W. Fetscher, B. D. Fields, B. Foster, A. Freitas, H. Gallagher, L. Garren, H. J. Gerber, G. Gerbier, T. Gershon, Y. Gershtein, T. Gherghetta, A. A. Godizov, M. C. Gonzalez-Garcia, M. Goodman, C. Grab, A. V. Gritsan, C. Grojean, M. Grünewald, A. Gurtu, T. Gutsche, H. E. Haber, C. Hanhart, S. Hashimoto, Y. Hayato, A. Hebecker, S. Heinemeyer, B. Heltsley, J. J. Hernández-Rey, K. Hikasa, J. Hisano, A. Höcker, J. Holder, A. Holtkamp, J. Huston, T. Hyodo, K. F. Johnson, M. Kado, M. Karliner, U. F. Katz, M. Kenzie, V. A. Khoze, S. R. Klein, E. Klempt, R. V. Kowalewski, F. Krauss, M. Kreps, B. Krusche, Y. Kwon, O. Lahav, J. Laiho, L. P. Lellouch, J. Lesgourgues, A. R. Liddle, Z. Ligeti, C. Lippmann, T. M. Liss, L. Littenberg, C. Lourengo, S. B. Lugovsky, A. Lusiani, Y. Makida, F. Maltoni, T. Mannel, A. V. Manohar, W. J. Marciano, A. Masoni, J. Matthews, U. G. Meißner, M. Mikhasenko, D. J. Miller, D. Milstead, R. E. Mitchell, K. Mönig, P. Molaro, F. Moortgat, M. Moskovic, K. Nakamura, M. Narain, P. Nason, S. Navas, M. Neubert, P. Nevski, Y. Nir, K. A. Olive, C. Patrignani, J. A. Peacock, S. T. Petcov, V. A. Petrov, A. Pich, A. Piepke, A. Pomarol, S. Profumo, A. Quadt, K. Rabbertz, J. Rademacker, G. Raffelt, H. Ramani, M. Ramsey-Musolf, B. N. Ratcliff, P. Richardson, A. Ringwald, S. Roesler, S. Rolli, A. Romaniouk, L. J. Rosenberg, J. L. Rosner, G. Rybka, M. Ryskin, R. A. Ryutin, Y. Sakai, G. P. Salam, S. Sarkar, F. Sauli, O. Schneider, K. Scholberg, A. J. Schwartz, J. Schwiening, D. Scott, V. Sharma, S. R. Sharpe, T. Shutt, M. Silari, T. Sjöstrand, P. Skands, T. Skwarnicki, G. F. Smoot, A. Soffer, M. S. Sozzi, S. Spanier, C. Spiering, A. Stahl, S. L. Stone, Y. Sumino, T. Sumiyoshi, M. J. Syphers, F. Takahashi, M. Tanabashi, J. Tanaka, M. Taševský, K. Terashi, J. Terning, U. Thoma, R. S. Thorne, L. Tiator, M. Titov, N. P. Tkachenko, D. R. Tovey, K. Trabelsi, P. Urquijo, G. Valencia, R. Van De Water, N. Varelas, G. Venanzoni, L. Verde, M. G. Vincter, P. Vogel, W. Vogelsang, A. Vogt, V. Vorobyev, S. P. Wakely, W. Walkowiak, C. W. Walter, D. Wands, M. O. Wascko, D. H. Weinberg, E. J. Weinberg, M. White, L. R. Wiencke, S. Willocq, C. L. Woody, R. L. Workman, M. Yokoyama, R. Yoshida, G. Zanderighi, G. P. Zeller, O. V. Zenin, R. Y. Zhu, S. L.

Zhu, F. Zimmermann, J. Anderson, T. Basaglia, V. S. Lugovsky, P. Schaffner, and W. Zheng, "Review of particle physics," vol. 2020, no. 8, p. 083C01.

[14] S. Adhikari, C. Akondi, H. Al Ghoul, A. Ali, M. Amaryan, E. Anassontzis, A. Austregesilo, F. Barbosa, J. Barlow, A. Barnes, E. Barriga, R. Barsotti, T. Beattie, J. Benesch, V. Berdnikov, G. Biallas, T. Black, W. Boeglin, P. Brindza, W. Briscoe, T. Britton, J. Brock, W. Brooks, B. Cannon, C. Carlin, D. Carman, T. Carstens, N. Cao, O. Chernyshov, E. Chudakov, S. Cole, O. Cortes, W. Crahen, V. Crede, M. Dalton, T. Daniels, A. Deur, C. Dickover, S. Dobbs, A. Dolgolenko, R. Dotel, M. Dugger, R. Dzhygadlo, A. Dzierba, H. Egiyan, T. Erbora, A. Ernst, P. Eugenio, C. Fanelli, S. Fegan, A. Foda, J. Foote, J. Frye, S. Furletov, L. Gan, A. Gasparian, A. Gerasimov, N. Gevorgyan, C. Gleason, K. Goetzen, A. Goncalves, V. Goryachev, L. Guo, H. Hakobyan, A. Hamdi, J. Hardin, C. Henschel, G. Huber, C. Hutton, A. Hurley, P. Ioannou, D. Ireland, M. Ito, N. Jarvis, R. Jones, V. Kakoyan, S. Katsaganis, G. Kalicy, M. Kamel, C. Keith, F. Klein, R. Kliemt, D. Kolybaba, C. Kourkoumelis, S. Krueger, S. Kuleshov, I. Larin, D. Lawrence, J. Leckey, D. Lersch, B. Leverington, W. Levine, W. Li, B. Liu, K. Livingston, G. Lolos, V. Lyubovit- skij, D. Mack, H. Marukyan, P. Mattione, V. Matveev, M. McCaughan, M. McCracken, W. McGinley, J. McIntyre, D. Meekins, R. Mendez, C. Meyer, R. Miskimen, R. Mitchell, F. Mokaya, K. Moriya, F. Nerling, L. Ng, H. Ni, A. Ostrovidov, Z. Papandreou, M. Patsyuk, C. Paudel, P. Pauli, R. Pedroni, L. Pentchev, K. Peters, W. Phelps, J. Pierce, E. Pooser, V. Popov, B. Pratt, Y. Qiang, N. Qin, V. Razmyslovich, J. Reinhold, B. Ritchie, J. Ritman, L. Robison, D. Romanov, C. Romero, C. Salgado, N. Sandoval, T. Satogata, A. Schertz, S. Schadmand, A. Schick, R. Schumacher, C. Schwarz, J. Schwiening, A. Semenov, I. Semenova, K. Seth, X. Shen, M. Shepherd, E. Smith, D. Sober, A. Somov, S. Somov, O. Soto, N. Sparks, M. Staib, C. Stanislav, J. Stevens, J. Stewart, I. Strakovsky, B. L. Sumner, K. Suresh, V. Tarasov, S. Taylor, L. Teigrob, A. Teymurazyan, A. Thiel, I. Tolstukhin, A. Tomaradze, A. Toro, A. Tsaris, Y. Van Haarlem, G. Vasileiadis, I. Vega, G. Visser, G. Voulgaris, N. Walford, D. Werthmüller, T. Whitlatch, N. Wickramaarachchi, M. Williams, E. Wolin, T. Xiao, Y. Yang, J. Zarling, Z. Zhang, Q. Zhou, X. Zhou, and B. Zihlmann, "The GlueX beamline and detector," vol. 987, p. 164807.

[15] M. Acciarri, P. Achard, O. Adriani, M. Aguilar-Benitez, J. Alcaraz, G. Alemanni, J. Allaby, A. Aloisio, M. G. Alviggi, G. Ambrosi, H. Anderhub, V. P. Andreev, T. Angelescu, F. Anselmo, A. Arefiev, T. Azemoon, T. Aziz, P. Bagnaia, A. Bajo, L. Baksay, A. Balandras, S. V. Baldew, S. Banerjee, S. Banerjee, A. Barczyk, R. Barillère, P. Bartalini, M. Basile, N. Batalova, R. Battiston, A. Bay, F. Becattini, U. Becker, F. Behner, L. Bellucci, R. Berbeco, J. Berdugo, P. Berges, B. Bertucci, B. L. Betev, S. Bhattacharya, M. Biasini, A. Biland, J. J. Blaising, S. C. Blyth, G. J. Bobbink, A. Böhm, L. Boldizsar, B. Borgia, D. Bourilkov, M. Bourquin, S. Braccini, J. G. Branson, F. Brochu, A. Buffini, A. Buijs, J. D. Burger, W. J. Burger, X. D. Cai, M. Capell, G. Cara Romeo, G. Carlino, A. M. Cartacci, J. Casaus, G. Castellini, F. Cavallari, N. Cavallo, C. Cecchi, M. Cerrada, F. Cesaroni, M. Chamizo, Y. H. Chang, U. K. Chaturvedi, M. Chemarin, A. Chen, G. Chen, G. M. Chen, H. F. Chen, H. S. Chen, G. Chiefari,

L. Cifarelli, F. Cindolo, C. Civinini, I. Clare, R. Clare, G. Coignet, N. Colino, S. Costantini, F. Cotorobai, B. de la Cruz, A. Csilling, S. Cucciarelli, T. S. Dai, J. A. van Dalen, R. D'Alessandro, R. de Asmundis, P. Déglon, A. Degré, K. Deiters, D. della Volpe, E. Delmeire, P. Denes, F. DeNotaristefani, A. De Salvo, M. Diemoz, M. Dierckxsens, D. van Dierendonck, C. Dionisi, M. Dittmar, A. Dominguez, A. Doria, M. T. Dova, D. Duchesneau, D. Dufournaud, P. Duinker, I. Duran, H. El Mamouni, A. Engler, F. J. Eppling, F. C. Erné, P. Extermann, M. Fabre, M. A. Falagan, S. Falciano, A. Favara, J. Fay, O. Fedin, M. Felcini, T. Ferguson, H. Fesefeldt, E. Fiandrini, J. H. Field, F. Filthaut, P. H. Fisher, I. Fisk, G. Forconi, K. Freudenreich, C. Furetta, Y. Galaktionov, S. N. Ganguli, P. Garcia-Abia, M. Gataullin, S. S. Gau, S. Gentile, N. Gheordanescu, S. Giagu, Z. F. Gong, G. Grenier, O. Grimm, M. W. Gruenewald, M. Guida, R. van Gulik, V. K. Gupta, A. Gurtu, L. J. Gutay, D. Haas, A. Hasan, D. Hatzifotiadou, T. Hebbeker, A. Hervé, P. Hidas, J. Hirschfelder, H. Hofer, G. Holzner, H. Hoorani, S. R. Hou, Y. Hu, I. Iashvili, B. N. Jin, L. W. Jones, P. de Jong, I. Josa-Mutuberrıa, R. A. Khan, M. Kaur, M. N. Kienzle-Focacci, D. Kim, J. K. Kim, J. Kirkby, D. Kiss, W. Kittel, A. Klimentov, A. C. König, M. Kopal, A. Kopp, V. Koutsenko, M. Kräber, R. W. Kraemer, W. Krenz, A. Krüger, A. Kunin, P. Ladron de Guevara, I. Laktineh, G. Landi, M. Lebeau, A. Lebedev, P. Lebrun, P. Lecomte, P. Lecoq, P. Le Coultre, H. J. Lee, J. M. Le Goff, R. Leiste, P. Levtchenko, C. Li, S. Likhoded, C. H. Lin, W. T. Lin, F. L. Linde, L. Lista, Z. A. Liu, W. Lohmann, E. Longo, Y. S. Lu, K. Lübelsmeyer, C. Luci, D. Luckey, L. Lugnier, L. Luminari, W. Lustermann, W. G. Ma, M. Maity, L. Malgeri, A. Malinin, C. Maña, D. Mangeol, J. Mans, G. Marian, J. P. Martin, F. Marzano, K. Mazumdar, R. R. McNeil, S. Mele, L. Merola, M. Meschini, W. J. Metzger, M. von der Mey, A. Mihul, H. Milcent, G. Mirabelli, J. Mnich, G. B. Mohanty, T. Moulik, G. S. Muanza, A. J. M. Muijs, B. Musicar, M. Musy, M. Napolitano, F. Nessi-Tedaldi, H. Newman, T. Niessen, A. Nisati, H. Nowak, R. Ofierzynski, G. Organtini, A. Oulianov, C. Palomares, D. Pandoulas, S. Paoletti, P. Paolucci, R. Paramatti, H. K. Park, I. H. Park, G. Passaleva, S. Patricelli, T. Paul, M. Pauluzzi, C. Paus, F. Pauss, M. Pedace, S. Pensotti, D. Perret-Gallix, B. Petersen, D. Piccolo, F. Pierella, M. Pieri, P. A. Piroué, E. Pistolesi, V. Plyaskin, M. Pohl, V. Pojidaev, H. Postema, J. Pothier, D. O. Prokofiev, D. Prokofiev, J. Quartieri, G. Rahal-Callot, M. A. Rahaman, P. Raics, N. Raja, R. Ramelli, P. G. Rancoita, R. Ranieri, A. Raspereza, G. Raven, P. Razis, D. Ren, M. Rescigno, S. Reucroft, S. Riemann, K. Riles, J. Rodin, B. P. Roe, L. Romero, A. Rosca, S. Rosier-Lees, J. A. Rubio, G. Ruggiero, H. Rykaczewski, S. Saremi, S. Sarkar, J. Salicio, E. Sanchez, M. P. Sanders, C. Schäfer, V. Schegelsky, S. Schmidt-Kaerst, D. Schmitz, H. Schopper, D. J. Schotanus, G. Schwering, C. Sciacca, A. Seganti, L. Servoli, S. Shevchenko, N. Shivarov, V. Shoutko, E. Shumilov, A. Shvorob, T. Siedenburg, D. Son, B. Smith, P. Spillantini, M. Steuer, D. P. Stickland, A. Stone, B. Stoyanov, A. Straessner, K. Sudhakar, G. Sultanov, L. Z. Sun, S. Sushkov, H. Suter, J. D. Swain, Z. Szillasi, T. Sztaricskai, X. W. Tang, L. Tauscher, L. Taylor, B. Tellili, C. Timmermans, S. C. C. Ting, S. M. Ting, S. C. Tonwar, J. Tóth, C. Tully, K. L. Tung, Y. Uchida, J. Ulbricht, E. Valente, G. Vesztergombi, I. Vetlitsky, D. Vicinanza, G. Viertel, S. Villa, M. Vivargent, S. Vlachos, I. Vodopianov, H. Vogel, H. Vogt, I. Vorobiev, A. A. Vorobyov, A. Vorvolakos, M. Wadhwa, W. Wallraff, M. Wang, X. L. Wang, Z. M. Wang, A. Weber, M. Weber,

P. Wienemann, H. Wilkens, S. X. Wu, S. Wynhoff, L. Xia, Z. Z. Xu, J. Yamamoto, B. Z. Yang, C. G. Yang, H. J. Yang, M. Yang, J. B. Ye, S. C. Yeh, A. Zalite, Y. Zalite, Z. P. Zhang, G. Y. Zhu, R. Y. Zhu, A. Zichichi, G. Zilizi, B. Zimmermann, and M. Zöller, "K0sk0s final state in two-photon collisions and implications for glueballs," vol. 501, no. 3, pp. 173–182.

[16] V. Mathieu, N. Kochelev, and V. Vento, "The physics of glueballs," vol. 18, no. 1, pp. 1–49. Publisher: World Scientific Publishing Co.

[17] The CLAS Collaboration, S. Chandavar, J. T. Goetz, K. Hicks, D. Keller, M. C. Kunkel, M. Paolone, D. P. Weygand, K. P. Adhikari, S. Adhikari, Z. Akbar, J. Ball, I. Balossino, L. Barion, M. Bashkanov, M. Battaglieri, I. Bedlinskiy, A. S. Biselli, W. J. Briscoe, W. K. Brooks, V. D. Burkert, F. Cao, D. S. Carman, A. Celentano, G. Charles, T. Chetry, G. Ciullo, L. Clark, P. L. Cole, M. Contalbrigo, V. Crede, A. D'Angelo, N. Dashyan, R. De Vita, E. De Sanctis, M. Defurne, A. Deur, C. Djalali, R. Dupre, H. Egiyan, A. El Alaoui, L. El Fassi, P. Eugenio, G. Fedotov, A. Filippi, A. Fradi, G. Gavalian, Y. Ghandilyan, G. P. Gilfoyle, F. X. Girod, D. I. Glazier, W. Gohn, E. Golovatch, R. W. Gothe, K. A. Griffioen, M. Guidal, L. Guo, K. Hafidi, H. Hakobyan, C. Hanretty, N. Harrison, M. Hattawy, D. Heddle, M. Holtrop, Y. Ilieva, D. G. Ireland, E. L. Isupov, D. Jenkins, S. Johnston, K. Joo, S. Joosten, M. L. Kabir, G. Khachatryan, M. Khachatryan, M. Khandaker, W. Kim, A. Klein, F. J. Klein, V. Kubarovsky, L. Lanza, P. Lenisa, K. Livingston, I. J. D. MacGregor, N. Markov, M. E. McCracken, B. McKinnon, C. A. Meyer, T. Mineeva, V. Mokeev, A. Movsisyan, C. Munoz Camacho, P. Nadel-Turonski, S. Niccolai, G. Niculescu, M. Osipenko, A. I. Ostrovidov, R. Paremuzyan, K. Park, E. Pasyuk, W. Phelps, O. Pogorelko, J. W. Price, Y. Prok, D. Protopopescu, B. A. Raue, M. Ripani, D. Riser, B. G. Ritchie, A. Rizzo, G. Rosner, F. Sabatié, C. Salgado, R. A. Schumacher, Y. G. Sharabian, A. Simonyan, I. Skorodumina, D. Sokhan, G. D. Smith, N. Sparveris, S. Stepanyan, I. I. Strakovsky, S. Strauch, M. Ungaro, E. Voutier, X. Wei, N. Zachariou, J. Zhang, and Z. W. Zhao, "Double $\{K\}_{S}^{0}$ photoproduction off the proton at CLAS," vol. 97, no. 2, p. 025203. Publisher: American Physical Society.

[18] "Proceedings, conférence internationale d'aix-en-provence sur les particules elémentaires: Aix-en-provence, france, sep 14-20, 1961."

[19] A. R. Erwin, G. A. Hoyer, R. H. March, W. D. Walker, and T. P. Wangler, "Experimental cross section for $\ensuremath{\pi}\ensuremath{\pi}\ensuremath{\rightarrow}k\overline{K}$," vol. 9, no. 1, pp. 34–36. Publisher: American Physical Society.

[20] G. Alexander, O. I. Dahl, L. Jacobs, G. R. Kalbfleisch, D. H. Miller, A. Rittenberg, J. Schwartz, and G. A. Smith, "Final-state interactions in the ${\ensuremath{\pi}}^{\ensuremath{-}}+p\ensuremath{\rightarrow}k+\overline{K}+n$ reaction," vol. 9, no. 11, pp. 460–464. Publisher: American Physical Society.

[21] D. J. Crennell, G. R. Kalbfleisch, K. W. Lai, J. M. Scarr, T. G. Schumann, I. O. Skillicorn, and M. S. Webster, "Observation of an enhancement in the $i=0$ ${{k}_{1}}^{0}{{k}_{1}}^{0}$ system at 1068 MeV," vol. 16, no. 22, pp. 1025–1029. Publisher: American Physical Society.

[22] R. I. Hess, O. I. Dahl, L. M. Hardy, J. Kirz, and D. H. Miller, "Low-mass $k\overline{K}$ systems produced in ${\ensuremath{\pi}}^{\ensuremath{-}}p$ interactions below 5 BeV/c," vol. 17, no. 21, pp. 1109–1112. Publisher: American Physical Society.

[23] O. I. Dahl, L. M. Hardy, R. I. Hess, J. Kirz, and D. H. Miller, "Strange-particle production in ${\ensuremath{\pi}}^{\ensuremath{-}}p$ interactions from $1.5 \mathrm{to} 4.2 \frac{\mathrm{BeV}}{c}$. i. three-and-more-body final states," vol. 163, no. 5, pp. 1377–1429. Publisher: American Physical Society.

[24] W. Beusch, W. E. Fischer, B. Gobbi, M. Pepin, E. Polgar, P. Astbury, G. Brautti, G. Finocchiaro, J. C. Lassalle, A. Michelini, K. M. Terwilliger, D. Websdale, and C. H. West, "Observation of resonance in the KO1ko1 system," vol. 25, no. 5, pp. 357–361.

[25] T. F. Hoang, D. P. Eartly, J. J. Phelan, A. Roberts, C. L. Sandler, S. Bernstein, S. Margulies, D. W. McLeod, T. H. Groves, N. N. Biswas, N. M. Cason, V. P. Kenney, J. M. Marraffino, J. T. McGahan, J. A. Poirier, and W. D. Shephard, "$k_{1}^{}{}{}_{}{}{}^{0}k_{1}^{}{}{}_{}{}{}^{0}$ threshold enhancement in ${\ensuremath{\pi}}^{\ensuremath{-}}p\ensuremath{\rightarrow}k_{1}^{}{}{}_{}{}{}^{0}k_{1}^{}{}{}_{}{}{}^{0}n$ at 4 and 5 GeV/c," vol. 21, no. 5, pp. 316–319. Publisher: American Physical Society.

[26] T. F. Hoang, D. P. Eartly, J. J. Phelan, A. Roberts, C. L. Sandler, S. Bernstein, S. Margulies, D. W. McLeod, T. H. Groves, N. N. Biswas, N. M. Cason, V. P. Kenney, J. M. Marraffino, J. T. McGahan, J. A. Poirier, and W. D. Shephard, "Investigation of ${\ensuremath{\pi}}^{\ensuremath{-}}p\ensuremath{\rightarrow}k_{1}^{}{}{}_{}{}{}^{0}k_{1}^{}{}{}_{}{}{}^{0}n$ at 4 and 5 GeV/c," vol. 184, no. 5, pp. 1363–1374. Publisher: American Physical Society.

[27] W. Beusch, A. Birman, D. Websdale, and W. Wetzel, "A new upper limit for the decay rate (f →)," vol. 60, no. 1, pp. 101–104.

[28] W. Wetzel, K. Freudenreich, F. X. Gentit, P. Muhlemann, W. Beusch, A. Birman, D. Websdale, P. Astbury, A. Harckham, and M. Letheren, "A study of → KKkk using an experiment on p → KS0ks0n at 8.9 GeV/c," vol. 115, no. 2, pp. 208–236.

[29] N. M. Cason, V. A. Polychronakos, J. M. Bishop, N. N. Biswas, V. P. Kenney, D. S. Rhines, W. D. Shephard, and J. M. Watson, "Observation of a new scalar meson," vol. 36, no. 25, pp. 1485–1488. Publisher: American Physical Society.

[30] V. A. Polychronakos, N. M. Cason, J. M. Bishop, N. N. Biswas, V. P. Kenney, D. S. Rhines, R. C. Ruchti, W. D. Shephard, M. J. Stangl, and J. M. Watson, "Study of the reaction ${\ensuremath{\pi}}^{\ensuremath{-}}p\ensuremath{\rightarrow}n{K}_{S}^{0}{K}_{S}^{0}$ at 6.0 and 7.0 GeV/c," vol. 19, no. 5, pp. 1317–1335. Publisher: American Physical Society.

[31] F. Barreiro, J. Diaz, J. B. Gay, R. J. Hemingway, S. O. Holmgren, M. J. Losty, B. Jongejans, J. C. Kluyver, G. G. G. Massaro, W. J. Metzger, H. G. Tiecke, J. J. M. Timmermans, P. Grossmann, and W. L. McDowell, "Production and decay properties of f(1514) in kp interactions at 4.2 GeV/*c*," vol. 121, no. 2, pp. 237–250.

[32] S. R. Gottesman, A. Fainberg, M. Goldberg, N. Horwitz, G. C. Moneti, D. P. Weygand, R. Whitman, S. M. Jacobs, L. E. Kirsch, S. C. Moore, P. E. Schmidt, C. J. Donaldson, H. A. Gordon, G. R. Morris, T. Davis, and B. T. Meadows, "Peripheral production and decay of ${K}_{S}^{0}{K}_{S}^{0}$ in the reaction ${\ensuremath{\pi}}^{\ensuremath{-}}p\ensuremath{\rightarrow}{K}_{S}^{0}{K}_{S}^{0}+\mathrm{neutrals}$ at 15.4 GeV/c," vol. 22, no. 7, pp. 1503–1512. Publisher: American Physical Society.

[33] A. Etkin, K. J. Foley, R. S. Longacre, W. A. Love, T. W. Morris, S. Ozaki, E. D. Platner, V. A. Polychronakos, A. C. Saulys, Y. Teramato, C. D. Wheeler, E. H. Willen, K. W. Lai, S. J. Lindenbaum, M. A. Kramer, U. Mallik, W. A. Mann, R. Merenyi, J. Marraffino, C. E. Roos, and M. S. Webster, "Amplitude analysis of the ${K}_{S}^{0}{K}_{S}^{0}$ system produced in the reaction ${\ensuremath{\pi}}^{\ensuremath{-}}p\ensuremath{\rightarrow}{K}_{S}^{0}{K}_{S}^{0}n$ at 23 GeV/c," vol. 25, no. 7, pp. 1786–1802. Publisher: American Physical Society.

[34] M. Althoff, R. Brandelik, W. Braunschweig, K. Gather, F. J. Kirschfink, K. Lübelsmeyer, H. U. Martyn, G. Peise, J. Rimkus, H. G. Sander, D. Schmitz, H. Siebke, D. Trines, W. Wallraff, H. Boerner, H. M. Fischer, H. Hartmann, E. Hilger, W. Hillen, G. Knop, L. Köpke, H. Kolanoski, H. Kück, R. Wedemeyer, N. Wermes, M. Wollstadt, H. Burkhardt, S. Cooper, J. Franzke, D. Hochman, H. Hultschig, P. Joos, W. Koch, U. Kötz, H. Kowalski, A. Ladage, B. Löhr, D. Lüke, P. Mättig, K. H. Mess, D. Notz, J. Pyrlik, D. R. Quarrie, R. Riethmüller, W. Schütte, P. Söding, G. Wolf, G. Yekutieli, R. Fohrmann, H. L. Krasemann, P. Leu, E. Lohrmann, D. Pandoulas, G. Poelz, P. Schmüser, B. H. Wiik, I. Al-Agil, R. Beuselinck, D. M. Binnie, A. J. Campbell, P. J. Dornan, B. Foster, D. A. Garbutt, T. D. Jones, W. G. Jones, J. McCardle, J. K. Sedgebeer, K. W. Bell, M. G. Bowler, I. C. Brock, R. J. Cashmore, R. Carnegie, P. E. L. Clarke, R. Devenish, P. Grossmann, J. Illingworth, S. L. Lloyd, G. L. Salmon, J. Thomas, T. R. Wyatt, C. Youngman, J. C. Hart, J. Harvey, J. Proudfoot, D. H. Saxon, P. L. Woodworth, D. Heyland, M. Holder, E. Duchovni, Y. Eisenberg, U. Karshon, G. Mikenberg, D. Revel, E. Ronat, A. Shapira, T. Barklow, M. Cherney, T. Meyer, G. Rudolph, H. Venkataramania, E. Wicklund, S. L. Wu, and G. Zobernig, "Production of

KK-pairs$k$ k-pairs in photon-photon collisions and the excitation of the tensor meson f(1515)," vol. 121, no. 2, pp. 216–222.

[35] R. S. Longacre, A. Etkin, K. J. Foley, W. A. Love, T. W. Morris, A. C. Saulys, E. D. Platner, S. J. Lindenbaum, J. R. Bensinger, L. E. Kirsch, H. Piekarz, R. A. Poster, J. Goo, M. A. Kramer, L. R. Fortney, A. T. Goshaw, E. McCrory, W. J. Robertson, J. M. Bishop, N. N. Biswas, N. M. Cason, V. P. Kenney, J. Piekarz, M. G. Rath, R. C. Ruchti, and W. D. Shephard, "A measurement of p→k0sk0sn at 22 GeV/c and a systematic study of the 2++ meson spectrum," vol. 177, no. 2, pp. 223–227.

[36] C. Berger and others, "Tensor meson excitation in the reaction \gamma \gamma \to k^0_s k^0_s," vol. 37, p. 329.

[37] D. Aston, N. Awaji, T. Bienz, F. Bird, J. D'Amore, W. Dunwoodie, R. Endorf, K. Fujii, H. Hayashii, S. Iwata, W. B. Johnson, R. Kajikawa, P. Kunz, D. W. G. S. Leith, L. Levinson, T. Matsui, B. T. Meadows, A. Miyamoto, M. Nussbaum, H. Ozaki, C. O. Pak, B. N. Ratcliff, D. Schultz, S. Shapiro, T. Shimomura, P. K. Sinervo, A. Sugiyama, S. Suzuki, G. Tarnopolsky, T. Tauchi, N. Toge, K. Ukai, A. Waite, and S. Williams, "A study of the ks0ks0 system in the reaction kp→ks0ks0 at 11 GeV/c," vol. 301, no. 4, pp. 525–553.

[38] H. J. Behrend, L. Criegee, J. B. Dainton, J. H. Field, G. Franke, H. Jung, J. Meyer, V. Schröder, G. G. Winter, P. J. Bussey, C. Buttar, A. J. Campbell, D. Hendry, G. McCurrach, J. M. Scarr, I. O. Skillicorn, K. M. Smith, J. Ahme, V. Blobel, W. Brehm, M. Feindt, H. Fenner, J. Harjes, J. H. Peters, O. Podobrin, H. Spitzer, W. D. Apel, J. Engler, G. Flügge, D. C. Fries, J. Fuster, P. Gabriel, K. Gamerdinger, J. Hansmeyer, H. Küster, H. Müller, K. H. Ranitzsch, H. Schneider, R. Seufert, W. de Boer, G. Buschhorn, G. Grindhammer, B. Gunderson, C. Kiesling, R. Kotthaus, H. Kroha, D. Lüers, H. Oberlack, P. Schacht, S. Scholz, G. Shooshtari, W. Wiedenmann, M. Davier, J. F. Grivaz, J. Haissinski, P. Janot, V. Journé, D. W. Kim, F. Le Diberder, J. J. Veillet, K. Blohm, R. George, M. Goldberg, O. Hamon, F. Kapusta, L. Poggioli, M. Rivoal, G. d'Agostini, F. Ferrarotto, M. Iacovacci, B. Stella, G. Cozzika, Y. Ducros, G. Alexander, A. Beck, G. Bella, J. Grunhaus, A. Klatchko, A. Levy, C. Milsténe, and CELLO Collaboration, "TheKS0ks0final state in interactions," vol. 43, no. 1, pp. 91–96.

[39] M. Acciarri, A. Adam, O. Adriani, M. Aguilar-Benitez, S. Ahlen, B. Alpat, J. Alcaraz, J. Allaby, A. Aloisio, G. Alverson, M. G. Alviggi, G. Ambrosi, Q. An, H. Anderhub, V. P. Andreev, T. Angelescu, D. Antreasyan, A. Arefiev, T. Azemoon, T. Aziz, P. V. K. S. Baba, P. Bagnaia, L. Baksay, R. C. Ball, S. Banerjee, K. Banicz, R. Barillère, L. Barone, P. Bartalini, A. Baschirotto, M. Basile, R. Battiston, A. Bay, F. Becattini, U. Becker, F. Behner, G. L. Bencze, J. Berdugo, P. Berges, B. Bertucci, B. L. Betev, M. Biasini, A. Biland, G. M. Bilei, R. Bizzarri, J. J. Blaising, G. J. Bobbink, R. Bock, A. Böhm, B. Borgia, A. Boucham, D. Bourilkov, M. Bourquin, D. Boutigny, S. Braccini, E. Brambilla, J. G. Branson, V. Brigljevic, I. C. Brock, A. Buijs, A. Bujak, J. D. Burger, W. J. Burger, C. Burgos, J. Busenitz, A. Buytenhuijs, X. D. Cai, M. Capell, G. Cara Romeo, M. Caria, G. Carlino, A. M. Cartacci, J. Casaus,

G. Castellini, R. Castello, F. Cavallari, N. Cavallo, C. Cecchi, M. Cerrada, F. Cesaroni, M. Chamizo, A. Chan, Y. H. Chang, U. K. Chaturvedi, M. Chemarin, A. Chen, C. Chen, G. Chen, G. M. Chen, H. F. Chen, H. S. Chen, M. Chen, G. Chiefari, C. Y. Chien, M. T. Choi, L. Cifarelli, F. Cindolo, C. Civinini, I. Clare, R. Clare, T. E. Coan, H. O. Cohn, G. Coignet, A. P. Colijn, N. Colino, V. Commichau, S. Costantini, F. Cotorobai, B. de la Cruz, X. T. Cui, X. Y. Cui, T. S. Dai, R. D'Alessandro, R. de Asmundis, H. De Boeck, A. Degré, K. Deiters, E. Dénes, P. Denes, F. DeNotaristefani, D. DiBitonto, M. Diemoz, D. van Dierendonck, F. Di Lodovico, C. Dionisi, M. Dittmar, A. Dominguez, A. Doria, I. Dorne, M. T. Dova, E. Drago, D. Duchesneau, P. Duinker, I. Duran, S. Dutta, S. Easo, Y. Efremenko, H. El Mamouni, A. Engler, F. J. Eppling, F. C. Erné, J. P. Ernenwein, P. Extermann, R. Fabbretti, M. Fabre, R. Faccini, S. Falciano, A. Favara, J. Fay, M. Felcini, T. Ferguson, D. Fernandez, G. Fernandez, F. Ferroni, H. Fesefeldt, E. Fiandrini, J. H. Field, F. Filthaut, P. H. Fisher, G. Forconi, L. Fredj, K. Freudenreich, M. Gailloud, Y. Galaktionov, S. N. Ganguli, P. Garcia-Abia, S. S. Gau, S. Gentile, J. Gerald, N. Gheordanescu, S. Giagu, S. Goldfarb, J. Goldstein, Z. F. Gong, E. Gonzalez, A. Gougas, D. Goujon, G. Gratta, M. W. Gruenewald, C. Gu, M. Guanziroli, V. K. Gupta, A. Gurtu, H. R. Gustafson, L. J. Gutay, B. Hartmann, A. Hasan, J. T. He, T. Hebbeker, A. Hervé, K. Hilgers, W. C. van Hoek, H. Hofer, H. Hoorani, S. R. Hou, G. Hu, M. M. Ilyas, V. Innocente, H. Janssen, B. N. Jin, L. W. Jones, P. de Jong, I. Josa-Mutuberria, A. Kasser, R. A. Khan, Y. Kamyshkov, P. Kapinos, J. S. Kapustinsky, Y. Karyotakis, M. Kaur, S. Khokhar, M. N. Kienzle-Focacci, D. Kim, J. K. Kim, S. C. Kim, Y. G. Kim, W. W. Kinnison, A. Kirkby, D. Kirkby, J. Kirkby, W. Kittel, A. Klimentov, A. C. König, E. Koffeman, O. Kornadt, V. Koutsenko, A. Koulbardis, R. W. Kraemer, T. Kramer, W. Krenz, H. Kuijten, A. Kunin, P. Ladron de Guevara, G. Landi, C. Lapoint, K. Lassila-Perini, P. Laurikainen, M. Lebeau, A. Lebedev, P. Lebrun, P. Lecomte, P. Lecoq, P. Le Coultre, J. S. Lee, K. Y. Lee, C. Leggett, J. M. Le Goff, R. Leiste, M. Lenti, E. Leonardi, P. Levtchenko, C. Li, E. Lieb, W. T. Lin, F. L. Linde, B. Lindemann, L. Lista, Y. Liu, Z. A. Liu, W. Lohmann, E. Longo, W. Lu, Y. S. Lu, K. Lübelsmeyer, C. Luci, D. Luckey, L. Ludovici, L. Luminari, W. Lustermann, W. G. Ma, A. Macchiolo, M. Maity, L. Malgeri, R. Malik, A. Malinin, C. Maña, S. Mangla, M. Maolinbay, P. Marchesini, A. Marin, J. P. Martin, F. Marzano, G. G. G. Massaro, K. Mazumdar, D. McNally, S. Mele, L. Merola, M. Meschini, W. J. Metzger, Y. Mi, A. Mihul, A. J. W. van Mil, Y. Mir, G. Mirabelli, J. Mnich, M. Möller, B. Monteleoni, R. Moore, R. Morand, S. Morganti, N. E. Moulai, R. Mount, S. Müller, F. Muheim, E. Nagy, S. Nahn, M. Napolitano, F. Nessi-Tedaldi, H. Newman, M. A. Niaz, A. Nippe, H. Nowak, G. Organtini, R. Ostonen, D. Pandoulas, S. Paoletti, P. Paolucci, G. Pascale, G. Passaleva, S. Patricelli, T. Paul, M. Pauluzzi, C. Paus, F. Pauss, Y. J. Pei, S. Pensotti, D. Perret-Gallix, S. Petrak, A. Pevsner, D. Piccolo, M. Pieri, J. C. Pinto, P. A. Piroué, E. Pistolesi, V. Plyaskin, M. Pohl, V. Pojidaev, H. Postema, N. Produit, K. N. Qureshi, R. Raghavan, G. Rahal-Callot, P. G. Rancoita, M. Rattaggi, G. Raven, P. Razis, K. Read, M. Redaelli, D. Ren, Z. Ren, M. Rescigno, S. Reucroft, A. Ricker, S. Riemann, B. C. Riemers, K. Riles, O. Rind, H. A. Rizvi, S. Ro, A. Robohm, J. Rodin, F. J. Rodriguez, B. P. Roe, M. Röhner, S. Röhner, L. Romero, S. Rosier-Lees, P. Rosselet, W. van Rossum, S. Roth, J. A. Rubio, H. Rykaczewski, J. Salicio,

J. M. Salicio, E. Sanchez, A. Santocchia, M. E. Sarakinos, S. Sarkar, G. Sartorelli, M. Sassowsky, G. Sauvage, C. Schäfer, V. Schegelsky, D. Schmitz, P. Schmitz, M. Schneegans, B. Schoeneich, N. Scholz, H. Schopper, D. J. Schotanus, R. Schulte, K. Schultze, J. Schwenke, G. Schwering, C. Sciacca, R. Sehgal, P. G. Seiler, J. C. Sens, L. Servoli, S. Shevchenko, N. Shivarov, V. Shoutko, J. Shukla, E. Shumilov, D. Son, A. Sopczak, V. Soulimov, B. Smith, T. Spickermann, P. Spillantini, M. Steuer, D. P. Stickland, F. Sticozzi, H. Stone, B. Stoyanov, K. Strauch, K. Sudhakar, G. Sultanov, L. Z. Sun, G. F. Susinno, H. Suter, J. D. Swain, X. W. Tang, L. Tauscher, L. Taylor, R. Timellini, S. C. C. Ting, S. M. Ting, O. Toker, F. Tonisch, M. Tonutti, S. C. Tonwar, J. Tóth, A. Tsaregorodtsey, G. Tsipolitis, C. Tully, H. Tuchscherer, J. Ulbricht, L. Urbán, U. Uwer, E. Valente, R. T. Van de Walle, I. Vetlitsky, G. Viertel, P. Vikas, U. Vikas, M. Vivargent, R. Völkert, H. Vogel, H. Vogt, I. Vorobiev, A. A. Vorobyov, A. A. Vorobyov, L. Vuilleumier, M. Wadhwa, W. Wallraff, J. C. Wang, X. L. Wang, Y. F. Wang, Z. M. Wang, A. Weber, R. Weill, C. Willmott, F. Wittgenstein, S. X. Wu, S. Wynhoff, J. Xu, Z. Z. Xu, B. Z. Yang, C. G. Yang, G. Yang, X. Y. Yao, C. H. Ye, J. B. Ye, Q. Ye, S. C. Yeh, J. M. You, N. Yunus, C. Zaccardelli, A. Zalite, P. Zemp, J. Y. Zeng, M. Zeng, Y. Zeng, Z. Zhang, Z. P. Zhang, B. Zhou, G. J. Zhou, J. F. Zhou, Y. Zhou, G. Y. Zhu, R. Y. Zhu, A. Zichichi, and B. C. C. van der Zwaan, "Study of the KS0ks0 final state in two-photon collisions," vol. 363, no. 1, pp. 118–126.

[40] M. A. Reyes, M. C. Berisso, D. C. Christian, J. Felix, A. Gara, E. Gottschalk, G. Gutierrez, E. P. Hartouni, B. C. Knapp, M. N. Kreisler, S. Lee, K. Markianos, G. Moreno, M. Sosa, M. H. L. S. Wang, A. Wehmann, and D. Wesson, "Partial wave analysis of the centrally produced ${K}_{S}{K}_{S}$ system at $800\phantom{\rule{0ex}{0ex}}GeV/\mathit{c}$," vol. 81, no. 19, pp. 4079–4082. Publisher: American Physical Society.

[41] B. P. Barkov, V. V. Vladimirskii, V. K. Grigor'ev, O. N. Erofeeva, Y. V. Katinov, I. Y. Korol'kov, V. I. Lisin, V. N. Luzin, V. N. Nozdrachev, V. V. Sokolovskii, G. D. Tikhomirov, S. A. Uzunyan, Y. P. Shkurenko, and I. A. Gridnev, "Discovery of a narrow resonance state of the system KSKSat mass 1520 MeV," vol. 70, no. 4, pp. 248–253.

[42] G. D. Tikhomirov, I. A. Erofeev, O. N. Erofeeva, and V. N. Luzin, "Resonances in the KSKSKLsystem produced in collisions of negative pions with a carbon target at a momentum of 40 GeV," vol. 66, no. 5, pp. 828–835.

[43] V. A. Schegelsky, A. V. Sarantsev, V. A. Nikonov, and A. V. Anisovich, "The k0 SK0 s final state in two-photon collisions and SU(3) tensor nonets," vol. 27, no. 2, pp. 207–212.

[44] V. V. Vladimirsky, V. K. Grigor'ev, I. A. Erofeev, O. N. Erofeeva, Y. V. Katinov, V. I. Lisin, V. N. Luzin, V. N. Nozdrachev, V. V. Sokolovsky, G. D. Tikhomirov, and Y. P. Shkurenko, "Analysis of the KSKS system from the reaction p → KSKSn at 40 GeV," vol. 69, no. 3, pp. 493–509.

[45] S. Uehara, Y. Watanabe, H. Nakazawa, I. Adachi, H. Aihara, D. M. Asner, V. Aulchenko, T. Aushev, A. M. Bakich, A. Bala, V. Bhardwaj, B. Bhuyan, A. Bondar, G. Bonvicini, A. Bozek, M. Bračko, V. Chekelian, A. Chen,

P. Chen, B. G. Cheon, K. Chilikin, R. Chistov, K. Cho, V. Chobanova, S.-K. Choi, Y. Choi, D. Cinabro, J. Dalseno, J. Dingfelder, Z. Doležal, D. Dutta, S. Eidelman, D. Epifanov, H. Farhat, J. E. Fast, M. Feindt, T. Ferber, A. Frey, V. Gaur, N. Gabyshev, S. Ganguly, R. Gillard, F. Giordano, Y. M. Goh, B. Golob, J. Haba, K. Hayasaka, H. Hayashii, Y. Hoshi, W.-S. Hou, H. J. Hyun, T. Iijima, A. Ishikawa, R. Itoh, Y. Iwasaki, T. Julius, D. H. Kah, J. H. Kang, E. Kato, H. Kawai, T. Kawasaki, C. Kiesling, D. Y. Kim, H. O. Kim, J. B. Kim, J. H. Kim, Y. J. Kim, J. Klucar, B. R. Ko, P. Kodyš, S. Korpar, P. Križan, P. Krokovny, T. Kumita, A. Kuzmin, Y.-J. Kwon, S.-H. Lee, J. Li, Y. Li, C. Liu, Z. Q. Liu, D. Liventsev, P. Lukin, D. Matvienko, K. Miyabayashi, H. Miyata, R. Mizuk, A. Moll, T. Mori, N. Muramatsu, R. Mussa, Y. Nagasaka, M. Nakao, C. Ng, K. N. Nisar, S. Nishida, O. Nitoh, S. Ogawa, S. Okuno, G. Pakhlova, C. W. Park, H. Park, H. K. Park, T. K. Pedlar, R. Pestotnik, M. Petrič, L. E. Piilonen, M. Ritter, M. Röhrken, A. Rostomyan, H. Sahoo, T. Saito, Y. Sakai, S. Sandilya, L. Santelj, T. Sanuki, V. Savinov, O. Schneider, G. Schnell, C. Schwanda, R. Seidl, K. Senyo, O. Seon, M. Shapkin, C. P. Shen, T.-A. Shibata, J.-G. Shiu, B. Shwartz, A. Sibidanov, F. Simon, Y.-S. Sohn, A. Sokolov, E. Solovieva, M. Starič, M. Steder, M. Sumihama, T. Sumiyoshi, U. Tamponi, K. Tanida, G. Tatishvili, Y. Teramoto, M. Uchida, T. Uglov, Y. Unno, S. Uno, P. Urquijo, S. E. Vahsen, C. Van Hulse, G. Varner, M. N. Wagner, C. H. Wang, M.-Z. Wang, P. Wang, X. L. Wang, K. M. Williams, E. Won, Y. Yamashita, S. Yashchenko, Y. Yook, C. Z. Yuan, Y. Yusa, C. C. Zhang, Z. P. Zhang, V. Zhilich, V. Zhulanov, A. Zupanc, and Belle Collaboration, "High-statistics study of k0s pair production in two-photon collisions," vol. 2013, no. 12, p. 123C01.

[46] A. Ali, F. Barbosa, J. Bessuille, E. Chudakov, R. Dzhygadlo, C. Fanelli, J. Frye, J. Hardin, A. Hurley, E. Ihloff, G. Kalicy, J. Kelsey, W. B. Li, M. Patsyuk, J. Schwiening, M. Shepherd, J. R. Stevens, T. Whitlatch, M. Williams, and Y. Yang, "Installation and commissioning of the GLUEX DIRC," vol. 15, no. 9, p. C09010.

[47] M. Pivk and F. Le Diberder, "sPlot: A statistical tool to unfold data distributions," vol. 555, no. 1, pp. 356–369.

[48] H. Dembinski, M. Kenzie, C. Langenbruch, and M. Schmelling, "Custom orthogonal weight functions (COWs) for event classification," vol. 1040, p. 167270.

[49] H. Akaike, "Information theory and an extension of the maximum likelihood principle," in *Selected Papers of Hirotugu Akaike* (E. Parzen, K. Tanabe, and G. Kitagawa, eds.), pp. 199–213, Springer.

[50] G. Schwarz, "Estimating the dimension of a model," vol. 6, no. 2, pp. 461–464. Publisher: Institute of Mathematical Statistics.